

JAERI-M  
86-173

PLASMA WALL INTERACTION IN OHMICALLY  
HEATED DISCHARGE OF JT-60 TOKAMAK

November 1986

Hiroo NAKAMURA, Toshiro ANDO, Setsuo NIKURA\*  
Takashi ARAI, Masahiro YAMAMOTO and JT-60 Team

JAERI-Mレポートは、日本原子力研究所が不定期に公刊している研究報告書です。

入手の問い合わせは、日本原子力研究所技術情報部情報資料課（〒319-11茨城県那珂郡東海村）あて、お申しこしてください。なお、このほかに財団法人原子力弘済会資料センター（〒319-11茨城県那珂郡東海村日本原子力研究所内）で複写による実費頒布をおこなっております。

JAERI-M reports are issued irregularly.

Inquiries about availability of the reports should be addressed to Information Division, Department of Technical Information, Japan Atomic Energy Research Institute, Tokai-mura, Naka-gun, Ibaraki-ken 319-11, Japan.

© Japan Atomic Energy Research Institute, 1986

---

編集兼発行	日本原子力研究所
印刷	日立高速印刷株式会社

PLASMA WALL INTERACTIONS IN OHMICALLY  
HEATED DISCHARGE OF JT-60 TOKAMAK

Hiroo NAKAMURA<sup>+</sup>, Toshiro ANDO, Setsuo NIIKURA\*  
Takashi ARAI, Masahiro YAMAMOTO and JT-60 Team<sup>++</sup>

Department of JT-60 Facility  
Naka Fusion Research Establishment  
Japan Atomic Energy Research Institute  
Naka-machi, Naka-gun, Ibaraki-ken

(Received October 20, 1986)

In this paper, the experimental results of plasma wall interactions in ohmically heated (OH) divertor and limiter discharges of JT-60 tokamak were described. In JT-60, all of the first wall have been coated by TiC of 20  $\mu\text{m}$  thick. Therefore, several interesting features were observed on discharge characteristics. High efficiency of Taylor type low current pulse discharge cleaning in JT-60 TiC coated wall was observed. Density control was possible even in a limiter discharge due to pumping ability of TiC wall. Heat load reduction by remote radiative cooling was observed in a divertor plate. Mo impurity was not observed in the JT-60 ohmic heating experiment except a plasma disruption. After the OH experiment, an observation of the first wall was carried out. Among 10000 pieces of the first wall components, severe melting of Mo substrate was observed only in a limiter at inboard side. In the pump limiter experiment, exhaust rate of 0.11  $\text{Pa}\cdot\text{m}^3/\text{sec}$  was obtained at  $\bar{n}_e = 2 \times 10^{19} \text{ m}^{-3}$ . Moreover, in the divertor pumping experiment, pressure in the divertor chamber increased in proportion to  $\bar{n}_e^2$ . A high pressure of 0.13 Pa was observed at  $\bar{n}_e = 6 \times 10^{19} \text{ m}^{-3}$ . Compression ratio was 40.

Keywords: Plasma Wall Interaction, JT-60, Ohmic Heating, Discharge Cleaning, Recycling, Energy Balance, Particle Balance, Remote Cooling, TiC Coated Mo, Melting, Pump limiter, Divertor Pumping system.

---

<sup>+</sup> Department of Large Tokamak Research.

\* on leave from Mitsubishi Atomic Power Industries, Inc.

++  
T.ABE, H.AIKAWA, N.AKAOKA, H.AKASAKA, M.AKIBA, N.AKINO, T.AKIYAMA, T.ANDO,  
K.ANNO, T.AOYAGI, T.ARAI, K.ARAKAWA, M.ARAKI, M.AZUMI, M.DAIRAKU, N.EBISAWA,  
T.FUJII, T.FUKUDA, T.FUKUDA, H.FURUKAWA, K.HAMAMATSU, T.HARAGUCHI, K.HAYASHI,  
H.HIRATSUKA, T.HIRAYAMA, K.IIDA, S.HIROKI, K.HIRUTA, N.HITOMI, M.HONDA,  
H.HORIIKE, R.HOSODA, N.HOSOGANE, H.ICHIGE, S.IIDA, T.IIJIMA, Y.IKEDA, T.IMAI,  
H.INAMI, N.ISAJI, M.ISAKA, M.ISHIHARA, H.ITOH, Y.ITOH, T.KANAI, T.KATOH,  
M.KAWAI, Y.KAWAMATA, Y.KIHARA, K.KAWASAKI, M.KIKUCHI, H.KIMURA, T.KIMURA,  
H.KISHIMOTO, K.KITAHARA, S.KITAMURA, A.KITSUNEZAKI, K.KIYONO, K.KODAMA,  
Y.KOIDE, T.KOIKE, M.KOMATA, I.KONDO, S.KONOSHIMA, H.KUBO, S.KUNIEDA,  
S.KURAKADA, K.KURIHARA, M.KURIYAMA, T.KURODA, M.MAENO, S.MATSUDA, M.MATSUKAWA,  
T.MATSUKAWA, M.MATSUO, M.MATSUOKA, N.MIYA, K.MIYACHI, Y.MIYO, K.MIZUHASHI,  
M.MIZUNO, Y.MURAKAMI, M.MUTOH, M.NAGAMI, A.NAGASHIMA, K.NAGASHIMA, S.NAGAYA,  
H.NAKAMURA, Y.NAKAMURA, T.NAGASHIMA, M.NEMOTO, Y.NEYATANI, S.NIIKURA,  
H.NINOMIYA, T.NISHITANI, T.NISHIYAMA, H.NOMATA, S.NOSHIROYA, N.OGIWARA,  
K.OHASA, T.OHGA, H.OHHARA, M.OHKUBO, K.OHMORI, S.OHMORI, Y.OHMORI, Y.OHSATO,  
T.OHSHIMA, M.OHTA, Y.OHARA, Y.OHUCHI, Y.OKUMURA, K.OTSU, A.OIKAWA, T.OZEKI,  
M.SAIGUSA, K.SAKAMOTO, A.SAKASAI, S.SAKATA, M.SATO, M.SAWAHATA, K.SHIBANUMA,  
T.SHIBATA, M.SEIMIYA, M.SEKI, S.SEKI, M.SHITOMI, R.SHIMADA, K.SHIMIZU,  
M.SHIMIZU, Y.SHIMOMURA, S.SHINOZAKI, H.SHIRAI, H.SHIRAKATA, K.SUGANUMA,  
T.SUGAWARA, T.SUGIE, H.SUNAOSHI, K.SUZUKI, M.SUZUKI, N.SUZUKI, S.SUZUKI,  
Y.SUZUKI, S.TAHIRA, M.TAKAHASHI, S.TAKAHASHI, T.TAKAHASHI, H.TAKATSU,  
Y.TAKAYASU, S.TAKEDA, H.TAKEUCHI, T.TAKIZUKA, S.TAMURA, E.TANAKA, S.TANAKA,  
T.TANAKA, K.TANI, T.TERAKADO, K.TOBITA, T.TOKUTAKE, T.TOTSUKA, N.TOYOSHIMA,  
T.TSUGITA, S.TSUJI, Y.TSUKAHARA, M.TSUNEOKA, K.UEHARA, M.UEHARA, K.UJIE,  
H.URAKAWA, Y.URAMOTO, K.USHIGUSA, K.USUI, K.WATANABE, J.YAGYU, K.YAMADA,  
M.YAMAMOTO, O.YAMASHITA, Y.YAMASHITA, K.YANO, K.YOKOKURA, H.YOKOMIZO,  
I.YONEKAWA, H.YOSHIDA, M.YOSHIKAWA, R.YOSHINO

## J T - 60のオーミック加熱放電におけるプラズマ・壁相互作用

日本原子力研究所那珂研究所 J T - 60試験部  
 中村博雄<sup>+</sup>・安東俊郎・新倉節夫<sup>\*</sup>・新井 貴  
 山本正弘・ J T - 60チーム<sup>++</sup>

( 1986年10月20日受理 )

J T - 60のオーミック加熱放電におけるプラズマ・壁相互作用に関する実験結果について述べた。J T - 60では、第1壁は、全て20  $\mu$ m厚さのTiCが被覆されている。そのため、放電洗浄・粒子バランス・エネルギーバランスおよび不純物等の実験結果に、興味有る特徴が見られた。TDC方式弱電流放電洗浄中の残留ガス分析によれば、主要ピークの大きさは、 $m/e = 16$  ( $\text{CH}_4$ ), 28 ( $\text{CO}/\text{C}_2\text{H}_4$ ), 18 ( $\text{H}_2\text{O}$ ) の順である。これは、従来のトカマク装置で、最大ピークが $m/e = 18$ であるのと大きな相違である。粒子バランスについては、リミタ放電においてもガスパフの制御により、プラズマ密度の制御が可能であることが明らかになった。また、エネルギーバランスの評価から、ダイバータ部でのリモートクーリングが確かめられた。PHAの測定により、プラズマディスラプション時以外には、Mo不純物は観測されなかった。実験後に、TiC被覆第1壁の健全性評価を行ない、損傷は、約1万個にも及ぶ第1壁中の、わずか1個であることが明らかになった。以上の結果は、TiC被覆されたMoとInconel 625第1壁のJ T - 60ジュール加熱実験での優れた性能を示している。また、粒子制御実験として、ポンプリミタ実験及びダイバータ排気実験を行なった。ポンプリミタ実験では、 $\bar{n}_e = 2 \times 10^{19} \text{m}^{-3}$ で、 $0.11 \text{ Pa} \cdot \text{m}^3/\text{sec}$ の排気量が得られた。また、ダイバータ排気実験では、ダイバータ室圧力 $P_{\text{div}}$ は $\bar{n}_e^2$ に比例し、 $\bar{n}_e = 6 \times 10^{19} \text{m}^{-3}$ で $P_{\text{div}} = 0.13 \text{ Pa}$ が得られた。現在、J T - 60装置とNBI/RF加熱装置との結合試験が行なわれており、1986年11月までに、初期加熱実験の結果が得られる予定である。

---

那珂研究所：〒311-02 茨城県那珂郡那珂町大字向山801-1

+ 臨界プラズマ研究部 臨界プラズマ実験室

\* 外来研究員 三菱原子力工業(株)

## 著者 5 人以外の J T - 60 チームリスト

阿部, 相川, 赤岡, 赤坂, 秋場, 秋野, 秋山, 安納, 青柳, 荒川, 荒木, 安積, 大楽, 海老沢, 藤井, 福田(武), 福田(輝), 古川, 浜松, 原口, 林, 平塚, 平山, 飯田, 広木, 蛭田, 人見, 本田, 堀池, 細田, 細金, 石毛, 飯田, 飯島, 池田, 今井, 井波, 伊佐治, 井坂, 石原, 伊藤(孝), 伊藤(康), 金井, 加藤, 河合, 川俣, 木原, 川崎, 菊池, 木村(晴), 木村(豊), 岸本, 北原, 北村, 狐崎, 清野, 児玉, 小出, 小池, 小又, 近藤, 木島, 久保, 国枝, 倉形, 栗原, 栗山, 黒田, 前野, 松田, 松川(誠), 松川(達), 松尾, 松岡, 宮, 宮地, 三代, 水橋, 水野, 村上, 武藤, 永見, 永島(孝), 永島(圭), 永谷, 中村(幸), 長島, 根本, 関谷, 二宮, 西谷, 西山, 野亦, 熊代谷, 萩原, 大麻, 大賀, 大原, 大久保, 大森(俊), 大森(憲), 大森(栄), 大里, 大島, 太田, 小原, 大内, 奥村, 大都, 及川, 小関, 三枝, 坂本, 逆井, 坂田, 佐藤, 沢島, 柴沼, 柴田, 清宮, 関(省), 関(正), 部, 嶋田, 清水(勝), 清水(正), 下村, 篠崎, 白井, 白形, 菅沼, 菅原, 杉江, 砂押, 鈴木(卓), 鈴木(康), 鈴木(正), 鈴木(國), 鈴木(紀), 田平, 高橋(実), 高橋(春), 高橋(虎), 高津, 高安, 武田, 竹内, 滝塚, 田村, 田中(恵), 田中(茂), 田中(竹), 谷, 寺門, 飛田, 徳竹, 戸塚, 豊島, 次田, 辻, 塚原, 恒岡, 上原(和), 上原(宗), 氏家, 浦川, 浦本, 牛草, 薄井, 渡辺, 柳生, 山田, 山下(修), 山下(幸), 矢野, 横倉, 横溝, 米川, 吉田, 吉川, 芳野

## Contents

1. Introduction .....	1
2. Experimental arrangement .....	2
3. Wall conditioning .....	3
3.1 Pre-conditioning .....	3
3.2 Discharge cleaning .....	3
4. Discharge characteristics .....	5
4.1 Operation regimes .....	5
4.2 Impurities .....	5
4.3 Energy balance .....	5
4.4 Particle balance .....	6
4.5 Disruption .....	6
5. Post-experiment analysis of TiC coated first wall .....	8
5.1 Overall observation .....	8
5.2 Surface and cross section analyses .....	8
6. Particle control experiment .....	10
6.1 Module pump limiter experiment .....	10
6.2 Divertor pumping experiment .....	11
7. Summary and Conclusion .....	12
Acknowledgement .....	12
References .....	13

## 目 次

1. 序 論	1
2. 実験装置	2
3. 壁の清浄化	3
3.1 前処理・ベーキング	3
3.2 放電洗浄	3
4. 放電特性	5
4.1 放電領域	5
4.2 不 純 物	5
4.3 エネルギーバランス	5
4.4 粒子バランス	6
4.5 ディスラプション	6
5. 実験後のTiC被覆第1壁の分析	8
5.1 全体の観察	8
5.2 表面および断面分析	8
6. 粒子制御実験	10
6.1 ポンプリミタ実験	10
6.2 ダイバータ排気実験	11
7. ま と め	12
謝 辞	12
参考文献	13



## 1. Introduction

JT-60 is a large tokamak device with a single null poloidal divertor. Main purposes of the JT-60 are to achieve a breakeven condition ( $\bar{n} \tau_E = 2-6 \times 10^{19} \text{ s} \cdot \text{m}^{-3}$  and  $\bar{T} = 5-10 \text{ keV}$ ) and to study the physical and technological aspects relevant to fusion reactor development.<sup>1)-3)</sup> Therefore, JT-60 first wall design must satisfy various requirements on high heat flux, impurity control and particle control.<sup>4)</sup> Details of JT-60 tokamak machine were reviewed in elsewhere.<sup>5),6)</sup> In JT-60, Mo was selected as a first wall material of toroidal fixed limiters, divertor plates and neutral beam armor plates where high heat load was expected.<sup>7)-9)</sup> On the other hand, Inconel 625 was applied to liners.<sup>10)</sup> For the purpose of impurity control, all surfaces of the Mo and Inconel 625 first walls were coated with TiC coating layer of 20  $\mu\text{m}$  thick.<sup>11)-14)</sup> JT-60 is a first tokamak with all TiC coated metal first wall. Therefore, several interesting features of discharge characteristics on discharge cleaning, energy balance, particle balance and impurities are expected. After completion of the tokamak system, JT-60 initial ohmic heating experiments was started in May 1985.<sup>15)</sup> During July ~ Dec. 1985, installations of new diagnostics, pump limiter and divertor pumping system were carried out. Also, the commissioning of the heating systems was carried out.<sup>16)-18)</sup> Second ohmic heating experiments were started in March 1986.<sup>19)</sup>

In this paper, the experimental results of plasma wall interactions in the ohmic heating experiments of limiter and divertor discharges with the all TiC coated first wall are summarized. In the following section, experimental arrangements are described. In section 3, wall conditioning characteristics are shown. Discharge characteristics on operation region, impurities, energy balance, particle balance and disruption are presented in section 4. In section 5, the results of post-experiment analysis of the TiC coated first wall are discussed. In section 6, particle control experiments by pump limiter and divertor pumping system are presented. Section 7 provides a summary.

## 2. Experimental arrangement

The major parameters of JT-60 are summarized in Table 1 and a cross-sectional view of the vacuum vessel is shown in Fig. 1.<sup>9)</sup> The vacuum vessel made of Inconel 625 has a structure of rigid rings and bellows welded alternately to make a full torus. The inner surfaces of the vacuum vessel is fully covered by the first walls consisting of toroidal fixed limiters (Mo), NBI armor plates (Mo), magnetic limiter plates (Mo) and liners (Inconel 625).<sup>9),10)</sup> All first wall were coated with titanium carbide of 20  $\mu\text{m}$  thick.<sup>11)-14)</sup> Three divertor coils are installed inside the vacuum vessel to produce a single null poloidal divertor configuration.<sup>20),21)</sup> Installation of the TiC coated Mo and Inconel 625 first wall has been completed in Nov. 1984. Fig. 2 shows photograph of the inside of the JT-60 vacuum vessel prior to the first plasma in April 1985. The vacuum vessel is bakable by electric heaters up to 350°C, and evacuated by four sets of turbomolecular pumps with liquid nitrogen cold traps. The pumping speed of the system is 29 m<sup>3</sup>/sec for H<sub>2</sub> at the pumping port inlets.<sup>22)</sup> The diagnostics and monitors which were equipped for the initial ohmic heating (OH-I) experiments during April 1985 ~ June 1985 are listed in Table 2. After the OH-I experiment, commissionings of NBI and RF heating systems and diagnostics were carried out during July 1985-Dec. 1985. Also, for the purpose of particle control study, a module pump limiter with TiC coated Mo head of 28 cm in diameter and four divertor pumping system with Zr/Al getter pumps<sup>23)</sup> were installed. Moreover, to reduce backflow conductance between main chamber and divertor room, baffle plates were attached in the gaps between the divertor coils and the vacuum vessel. Also, the augmentation plates were attached to four ports of the torus main pumps in order to enhance the particle flow to the main pumps. In March 1986, the ohmic heating experiment was started again to obtain a target plasma for additional heating experiments by the NBI and RF systems.

### 3. Wall conditioning<sup>24)</sup>

#### 3.1 Pre-conditioning

The installation of the vacuum vessel was started in May 1983. The vacuum vessel, transported from the industry to the site, was divided into two semicircular vacuum vessels, each of which contained three half turn of all divertor coils. Careful vacuum quality control had been carried out during the course of installation.<sup>25)</sup> Clean air was forced into the vacuum vessel through an air filter. The density of dust particles was measured periodically. As a result, the number of dust particles inside the vacuum vessel was kept to be a few thousands per cubic feet. The inner surface of the vacuum vessel was cleaned by a vacuum cleanser, forced air, hot water or freon jet, and was wiped with special cloths wetted by freon or acetone, as shown in table 3. Special attention was paid to keep cleanlinesses of the delicate components such as all metal gate valves and first wall after the completion of the internal works. Baking tests were carried out three times as shown in table 3 in order to confirm the performance of the vacuum vessel during the baking and to improve vacuum quality. Final vacuum pressure of  $7.4 \times 10^{-7}$  Pa and outgassing rate of  $6.8 \times 10^{-10}$  Pa·m<sup>3</sup>/s·m<sup>2</sup> were obtained after the above bakings.

#### 3.2 Discharge cleaning

Taylor type low current pulse discharge cleaning (TDC) was performed under the conditions as shown in Table 4. Optimization of the discharge cleaning were made by varying gas feed rate, toroidal magnetic field, vertical magnetic field, discharge current and temperature of the vacuum vessel. Typical discharge conditions were derived from the above results. The plasma current of 30 kA was discharged for 40 ms at the toroidal field of 0.45 T and the gas feed rate of around 1.0 Pa·m<sup>3</sup>/s. A repetition period in the range from 1.2 s to 2.0 s was often chosen in the discharge cleaning from a viewpoint of allowable limit of temperature difference between the rigid ring and the bellows. Discharge cleaning in May 1985 was carried out for 30 hr about 200°C (1st TDC) and for 52 hr at room temperature (2nd TDC).

## 4. Discharge characteristics

### 4.1 Operation regimes

Typical experimental discharges in both limiter and divertor configurations are summarized in the  $I_p$ - $\bar{n}_e$  diagram of Fig. 6 and in the Hugill diagram of Fig. 7. In these figures, the results in the first ohmic experiment (April ~ June, 1986) and the second one (March-July, 1986) are shown. In the divertor discharge, the highest plasma parameters in the OH experiment were plasma current of 2 MA and plasma density of  $5.7 \times 10^{19} \text{ m}^{-3}$ . In the '86 OH experiment, maximum pulse length was extended from 5 sec in the '85 OH experiment to 10 sec. Typical wave forms of the 10 sec discharge is shown in Fig. 8. In the current ramp-up phase when  $q_{\text{eff}}$  crossed near an integer, loop voltage spikes was observed. The spikes around  $q_{\text{eff}}=3$  were associated with a rapid increase in  $H_\alpha$  intensity in the divertor plasma<sup>26)</sup>. In the ohmic plasmas, energy confinement time showed a slight dependence on  $\bar{n}_e$  for  $\bar{n}_e \geq 2 \times 10^{19} \text{ m}^{-3}$ . At  $\bar{n}_e > 2 \times 10^{19} \text{ m}^{-3}$ , energy confinement time was about 0.4 sec.

### 4.2 Impurities

The effective charge at the plasma center  $Z_{\text{eff}}(0)$  decreases with increasing  $\bar{n}_e$  and increases with the plasma current  $I_p$ . In  $\bar{n}_e \geq 3 \times 10^{19} \text{ m}^{-3}$ ,  $Z_{\text{eff}}$  is about 1 at  $I_p=1 \text{ MA}$  and 1.5 at  $I_p=1.5 \text{ MA}$ . Figure 9 shows the spectrum of soft X rays emitted from the main plasma in the divertor discharge.<sup>15)</sup> In the spectrum, the  $K_\alpha$ ,  $K_\beta$ ,  $K_\gamma$  lines of titanium were observed. However, no significant lines of molybdenum were observed except during a disruption. These results show that impurity contamination of molybdenum was suppressed by the TiC coating layer in the ohmic experiment.

### 4.3 Energy balance<sup>5)</sup>

During the first OH experiment (April ~ June 1985), global energy balance was investigated. The radiated powers from the main and

divertor plasmas were measured by bolometers (4-ch; main plasma, 1-ch; divertor plasma). Total deposition heat load on the divertor plates was measured by the thermocouples mechanically attached on the back of the divertor plates with the assumption of adiabatic condition. Figure 10 shows the accountability of the energy balance of the divertor discharge.<sup>27)</sup> The ohmic input energy is well accounted. About 70 % of the input energy is exhausted into the divertor room. About 50 % of the exhausted energy is radiated in the divertor room. Therefore, it is concluded that heat load to the divertor plate is reduced also in JT-60 by the remote radiative cooling observed in D-III.<sup>28),29)</sup> This remote radiative cooling mitigates the high heat load and the erosion problems in large tokamaks.

#### 4.4 Particle balance

Global particle balance of ohmically heated discharge was investigated by  $H_{\alpha}$  measurement, plasma density and gas flow.<sup>30)</sup> Time integrated fueling efficiency  $\eta$  is defined as a trapping ratio in the plasma of injected gas during a discharge. Therefore,  $\eta$  is obtained by an equation of  $\int n_e dV / \int Q dt$ . The fueling efficiency  $\eta$  is about 0.1 for the divertor discharge and about 0.2 for the limiter discharge, as shown in Fig. 11. Such a low value of  $\eta$  implies that a major part of the injected hydrogen is trapped in the TiC surface. After a discharge, the trapped gas was released during an interval of the discharges as shown in Fig. 12. Total number of the released particles during 12 min after a discharge is 40 ~ 80 % of the total number of the injected gas. As a result, density control is possible by a control of gas injection rate even in the limiter discharge. This is one of advantages of the TiC coated first wall.

#### 4.5 Disruption

To obtain a data base on disruption properties, the current decay rate during a disruption as a function of the plasma current was summarized. Heat load during a disruption is discussed in section 5. Among 325 shots during the first OH experiment (April ~ June 1986), the

number of the disruption shots was 59. Figure 13 shows the current decay rate of disruptions during the first OH experiment.<sup>15)</sup> There is no clear difference between divertor and limiter discharges. The highest current decay rate is about 125 MA/s. Also, a current decay time is 10-40 ms. These values are less than the design value of the divertor coil liner, where a permissible current decay time is 5 msec for a plasma current of 2.7 MA. This condition corresponds to a current decay rate of 380 MA/sec. In the ohmic heating experiment, it is concluded that a current decay time and decay rate are within the design value of the JT-60 first wall. In future, a data base on plasma disruption in additional heating experiment is necessary.

## 5. Post experiment analysis of TiC coated first wall

### 5.1 Overall observation

After the joule experiment during April 1985 - June 1985, visual inspection of the TiC coated first wall was carried out inside the vacuum vessel. As a result, a part of the first wall was exchanged to new one. Figure 14 shows a photograph of the first wall and in-vessel components after the ohmic heating experiment. In this photograph, several interesting features produced through plasma-wall interactions can be observed. First, significant discolorations of the TiC surface were observed in the liner attached around the divertor coils and in the fixed limiter and the protection plate attached in the large major radius side. The cause of these discolorations is not identified yet. However, similar discoloration can be caused by heating in a vacuum where oxygen exists. Therefore, it is expected that these discolorations were produced by the heat deposition during the discharge cleaning or the tokamak discharge. Secondly, on the surfaces of the toroidal fixed limiter, a pattern of slight discoloration can be seen. In this case, color of the TiC surface changed from gray to silver gray. This color change indicates the distribution of heat deposition.

Thirdly, in Fig. 14, severe melting of the Mo substrate was observed in the toroidal fixed limiter at inner-side of the torus. Total number of the severe melting was only one among about 10000 pieces of the first wall components. Cause of the severe melting is considered to be a high heat load during a runaway discharge or/and a disruption. This is discussed further in section 5.2. In this sector of the vacuum vessel, local meltings at the limiter edge were observed in upper and inner-side. In other sectors, the local meltings were observed in several limiters. Total number of these local meltings were only 10 among 1354 pieces of the toroidal fixed limiters.

### 5.2 Surface and cross section analyses

Figure 15 shows SEM micrograph and EPMA X-ray image of the local melted area. SEM micrograph shows exfoliation and microcracking of TiC

layer. Also, a droplet is observed. EPMA result shows the droplet of Mo and exfoliation of TiC layer. Further studies on surface analyses by AES, EPMA and so on are now under investigation. Figure 16 shows micrograph of cross section in the melted region. In Fig. 16, although TiC layer is not observed, dendritic structure of Mo and TiC is observed. Similar structure was also observed in high heat load experiment of TiC coated Mo specimen by an electron beam heating.<sup>31)-33)</sup> Below the dendritic structure, significant recrystallization of Mo is observed with a thickness of about 300  $\mu\text{m}$ . Considering the dendritic structure and the thickness of Mo recrystallization, high heat load with a short deposition time is expected. With a simple equation of  $t=d^2/(\lambda/C_p\rho)$ , a rough estimation of the deposition time is possible, where  $t$  is a deposition time,  $d$  is a thickness of Mo recrystallization zone,  $\lambda$  is a thermal conductivity of Mo,  $C_p$  is a specific heat of Mo, and  $\rho$  is a density of Mo. Using  $d=0.03$  cm,  $\lambda=0.28$  cal/cm $\cdot$ sec $\cdot$ °C,  $C_p=0.068$  cal/g $\cdot$ °C and  $\rho=10.2$  g/cm<sup>3</sup>, a deposition time is estimated to be a few msec. Such a short deposition time shows that the melting of Mo was caused by the heat load during a plasma disruption and/or a runaway electron discharge. In JT-60, surface temperature of the limiter during a disruption was not measured. However, to do rough estimation of the heat flux during a disruption, maximum surface temperature is assumed to be 2600°C, melting point of Mo. As a result, the heat flux is calculated to be a several tens kW/cm<sup>2</sup>. Detailed analyses on the above results are now under investigation.



## 6. Particle control experiment

### 6.1 Module pump limiter experiment

To investigate the pump limiter characteristics in a large tokamak, a module pump limiter experiment was carried out in JT-60 ohmically heated discharge (March 1985). The limiter head is 27 cm in diameter and consisted of molybdenum blades coated by 20  $\mu\text{m}$  thick TiC layer. The head has one entrance throat with a collection window of 1.0 cm in height and 18 cm in width. Figure 17 shows a photograph of the pump limiter head. Five Zr/Al getter pump modules (SAES C-500) were installed behind 5 m from the head. Effective pumping speed at the limiter head is 620 l/sec for  $\text{H}_2$ . The pressure in the pump limiter head is measured with a modified penning gauge. Electron densities and temperatures in the throat region and neutrallizer plate are measured by the Langmuir probes. Brazed thermocouples are attached to measure the heat load on the limiter blades and the neutrallizer plates. In the pump limiter experiment, a 1 MA plasma was produced with a contact of the inboard limiter and shifted to the pump limiter head as shown in Fig. 18. After the pump limiter discharge of 1 sec, a plasma shifted again to the inboard limiter. Figure 19 shows dependences of the pressure inside the limiter head and the exhausted gas  $Q_{\text{H}_2}$  on the line-averaged plasma density in the following two conditions. In the case A, a plasma contacted with only the pump limiter head. In the case B, a plasma contacted with the inboard limiter in addition to the pump limiter head. Case A shows strong dependence of  $P_{\text{H}_2}$  and  $Q_{\text{H}_2}$  on  $\bar{n}_e^{\text{C}}$  than the case B.  $Q_{\text{H}_2}$  and  $P_{\text{H}_2}$  increase in proportion to  $\bar{n}_e^{1-2}$ . At the highest density of  $2 \times 10^{19} \text{ m}^{-3}$ ,  $P_{\text{H}_2}$  is about 0.2 Pa and  $Q_{\text{H}_2}$  is 0.11  $\text{Pa} \cdot \text{m}^3/\text{sec}$ . Results of the Langmuir probe measurements showed significant increase of plasma density and decrease of plasma temperature near the neutrallizer plate with increase of main plasma density. These results show that an enhancement of recycling is expected near the neutrallizer plate.

6.2 Divertor pumping experiment<sup>23)</sup>

The objective of this system is an active particle control in neutral beam heated divertor discharges. The pumps are composed of four Zr/Al getter pumps with a pumping speed of 5.3 m<sup>3</sup>/s for H<sub>2</sub> in the divertor chamber. The pressures in the divertor and main chambers, the getter pump chamber and the manifold of the torus main pumps were measured by shielded ionization gauges during discharges. In addition, the particle flow from the divertor chamber to torus main pumps was enhanced by attaching augmentation plates inside the vacuum vessel. Baffle plates were also attached to reduce the conductance between the divertor and the main chambers. Figure 20 shows a typical divertor discharge with a plasma current ( $I_p$ ) of 2 MA and a pulse length of about 10 s. The line averaged electron density  $\bar{n}_e$  of the main plasma increases almost linearly with a constant gas injection rate ( $Q_{\text{gas}}$ ), while the pressure in the divertor chamber increases nonlinearly. The measured pressures in the divertor chamber ( $P_{\text{div}}$ ), in the main chamber ( $P_{\text{main}}$ ) and in the manifold of the torus main pumps ( $P_v$ ) are shown in Fig. 21 as a function of  $\bar{n}_e$  for the discharges with  $I_p=1.5 - 2$  MA and a pulse length of 10 s.  $P_{\text{div}}$  increases approximately in proportion to  $\bar{n}_e^2$  in the range from  $2 \times 10^{19}$  to  $6 \times 10^{19}$  m<sup>-3</sup>.  $P_{\text{main}}$  and  $P_v$  have also the same dependence on  $\bar{n}_e$ . The ratio of  $P_{\text{div}}$  to  $P_{\text{main}}$  is about 40, which indicates that a strong compression is achieved in the divertor chamber. For instance, at  $\bar{n}_e=6 \times 10^{19}$  m<sup>-3</sup>,  $P_{\text{div}}=0.13$  Pa, whereas  $P_{\text{main}}=0.0035$  Pa. Figure 22 shows the gas exhaust rates by the getter pumps ( $Q_{\text{Z/A}}$ ) and the four main pumps ( $Q_{\text{TMP}}$ ) as a function of  $\bar{n}_e$ .  $Q_{\text{Z/A}}$  and  $Q_{\text{TMP}}$  increase in proportion to  $\bar{n}_e^2$  as well. The fueling rates by the neutral beam injections with a heating power of 20 MW are 3 Pa·m<sup>3</sup>/sec and 2.3 Pa·m<sup>3</sup>/sec for beam energies of 75 keV and 100 keV, respectively. If the above dependence of the exhaust rate on  $\bar{n}_e$  is assumed to be applicable to a NBI heated experiment, the getter pumps are expected to exhaust 1.8 Pa·m<sup>3</sup>/sec and the torus main pumps exhaust 0.6 Pa·m<sup>3</sup>/sec at  $\bar{n}_e=1 \times 10^{20}$  m<sup>-3</sup>. The total gas exhaust rate is 2.4 Pa·m<sup>3</sup>/sec, which is as large as the fueling rate by the neutral beam injection. Further study in the NBI heated experiment is necessary.

## 7. Summary and conclusion

In the ohmically heated hydrogen discharge, the results are summarized as follows;

- (1) High efficiency of Taylor type low current pulse discharge cleaning in JT-60 TiC coated wall was observed.
- (2) Density control was possible even in a limiter discharge due to pumping ability of TiC wall.
- (3) Heat load reduction by remote radiative cooling was observed in a divertor plate.
- (4) Mo impurity was not observed in the JT-60 ohmic heating experiment except a plasma disruption.
- (5) Current decay rate and decay time during a plasma disruption were less than the design value of JT-60 first wall.
- (6) Post-experiment analysis of the first wall showed that among 10000 pieces of the first wall component, number of severe damage was only one in a limiter at inboard side.
- (7) Exhaust rate of  $0.11 \text{ Pa}\cdot\text{m}^3/\text{sec}$  and maximum pressure of  $0.2 \text{ Pa}$  were obtained at  $\bar{n}_e = 2 \times 10^{19} \text{ m}^{-3}$  in the pump limiter experiment.
- (8) The pressure in the divertor chamber increased approximately in proportion to the square of  $\bar{n}_e$ . A high pressure of  $0.13 \text{ Pa}$  was observed at  $\bar{n}_e = 6 \times 10^{19} \text{ m}^{-3}$ . Compression ratio was 40.

These results show that performances of the TiC coated Mo and Inconel first wall is quite well in the JT-60 ohmic heating experiment. Also, active density controls by a pump limiter and a divertor pumping system are possible. Linkage test between the additional heating systems and JT-60 system was started in Aug. 1986. Initial results of NBI and RF heated discharges will be shown until Nov. 1986.<sup>34)-36)</sup>

## Acknowledgements

The authors wish to thank the members of JAERI who have contributed to the JT-60 project throughout its progress. We also wish to express our gratitude to Drs. S. Mori, Y. Iso, and K. Tomabechi for their continued encouragements and supports.

## 7. Summary and conclusion

In the ohmically heated hydrogen discharge, the results are summarized as follows;

- (1) High efficiency of Taylor type low current pulse discharge cleaning in JT-60 TiC coated wall was observed.
- (2) Density control was possible even in a limiter discharge due to pumping ability of TiC wall.
- (3) Heat load reduction by remote radiative cooling was observed in a divertor plate.
- (4) No impurity was not observed in the JT-60 ohmic heating experiment except a plasma disruption.
- (5) Current decay rate and decay time during a plasma disruption were less than the design value of JT-60 first wall.
- (6) Post-experiment analysis of the first wall showed that among 10000 pieces of the first wall component, number of severe damage was only one in a limiter at inboard side.
- (7) Exhaust rate of  $0.11 \text{ Pa}\cdot\text{m}^3/\text{sec}$  and maximum pressure of  $0.2 \text{ Pa}$  were obtained at  $\bar{n}_e = 2 \times 10^{19} \text{ m}^{-3}$  in the pump limiter experiment.
- (8) The pressure in the divertor chamber increased approximately in proportion to the square of  $\bar{n}_e$ . A high pressure of  $0.13 \text{ Pa}$  was observed at  $\bar{n}_e = 6 \times 10^{19} \text{ m}^{-3}$ . Compression ratio was 40.

These results show that performances of the TiC coated Mo and Inconel first wall is quite well in the JT-60 ohmic heating experiment. Also, active density controls by a pump limiter and a divertor pumping system are possible. Linkage test between the additional heating systems and JT-60 system was started in Aug. 1986. Initial results of NBI and RF heated discharges will be shown until Nov. 1986.<sup>34)-36)</sup>

## Acknowledgements

The authors wish to thank the members of JAERI who have contributed to the JT-60 project throughout its progress. We also wish to express our gratitude to Drs. S. Mori, Y. Iso, and K. Tomabechi for their continued encouragements and supports.

## References

- [1] M. Yoshikawa, 6th Topical Meeting on the Technology of Fusion Energy, San Francisco, March 1985.
- [2] M. Yoshikawa and K. Tomabechi, Nuclear Technology/Fusion 4 (1983) 299.
- [3] Y. Shimomura et al., J. Nucl. Mater 128&129 (1984) 19.
- [4] H. Nakamura and Y. Murakami, Proc. IAEA Technical Committee Meeting on Divertors and Impurity Control, Garching, July 1981, 91.
- [5] Y. Iso and M. Ohta, Trans. of the 6th SMIRT, N(1981) 9.
- [6] M. Ohta et al., To be published in Nucl. Engineering and Design/Fusion.
- [7] H. Nakamura et al., Proc. 7th Symp. on Engineering Problems of Fusion Research, Knoxville, 1977, 1669.
- [8] H. Nakamura et al., To be published in J. Nucl. Science and Technology.
- [9] H. Nakamura et al., JAERI-M 84-062 (1984).
- [10] H. Nakamura et al., Proc. 11th Symp. on Fusion Technology, Sept. 1980, 1022.
- [11] H. Nakamura et al., Proc. US-Japan Workshop on Divertors, First Wall Materials and Impurity Control, Tokai, 1980. JAERI-M 8921 (1980) paper 10-2.
- [12] Y. Murakami et al., J. Nucl. Mater. 111&112 (1982) 861.
- [13] T. Abe et al., J. Nucl. Mater. 133&134 (1985) 254.
- [14] H. Nakamura et al., JAERI-M 85-022 (1985).
- [15] JT-60 Team (presented by M. Yoshikawa), Plasma Physics and Controlled Fusion, 28 (1986) 165.
- [16] Y. Ohara et al., Proc. 13th Symp. on Fusion Technology, Varese, Sept. 1984.
- [17] T. Nagashima et al., Proc. 10th Symp. on Fusion Engineering, Philadelphia, Oct. 1983.
- [18] JT-60 Team (presented by S. Tamura), Plasma Physics and Controlled Fusion, 28 (1980) 1377.
- [19] JT-60 Team (presented by H. Kishimoto), to be published in Proc. 7th Inter. Conf. on Plasma Surface Interaction, Princeton, May 1986.

- [20] R. Yoshino et al., Proc. 13th Symp. on Fusion Technology, Varese, Sept. 1984.
- [21] H. Ninomiya et al., Proc. 11th Symp. on Fusion Engineering, Austin, Nov. 1985, Vol. I, 518 and JAERI-M 86-110 (1986) (in Japanese).
- [22] N. Ogiwara et al., 13th Symp. on Fusion Technology, Varese, Sept. 1984.
- [23] T. Ando et al., Proc. 14th Symp. on Fusion Technology, Avignon, Sept. 1986.
- [24] T. Arai et al., to be published in Proc. 7th Inter. Conf. on Plasma Surface Interaction, Princeton, May 1986.
- [25] M. Yamamoto et al., Proc. 11th Symp. on Fusion Engineering, Austin, Nov. 1985, Vol. I, 834.
- [26] JT-60 Team (presented by S. Tsuji), Proc. 12th European Conference on Controlled Fusion and Plasma Physics, Part I, 375.
- [27] Y. Koide et al., JAERI-M 86-056 (1986).
- [28] N. Maeno et al., Nucl. Fusion 21 (1981) 1474.
- [29] M. Shimada et al., Nucl. Fusion 22 (1982) 643.
- [30] K. Yamada et al., JAERI-M 86-057 (1986).
- [31] M. Onozuka et al., Proc. 11th Symp. on Fusion Engineering, Austin, Nov. 1985, Vol. 2, 920.
- [32] H. Nakamura et al., JAERI-M 86-048 (1986)(in Japanese).
- [33] M. Onozuka et al., To be published in Proc. 14th Symp. on Fusion Technology.
- [34] M. Yoshikawa et al., To be published in Proc. of 11th Inter. Conf. on Plasma Physics and Controlled Fusion, IAEA-CN-47/A-I-1, Kyoto, Nov. 1986.
- [35] JT-60 Team (presented by M. Nagami), To be published in Proc. of 11th Inter. Conf. on Plasma Physics and Controlled Fusion, IAEA-CN-47/A-II-2, Kyoto, Nov. 1986.
- [36] JT-60 Team (presented by H. Takeuchi), To be published in Proc. of 11th Inter. Conf. on Plasma Physics and Controlled Fusion, IAEA-CN-47/A-IV-3, Kyoto, Nov. 1986.

**Table 1** Major Parameters

Major Radius	3.0	m
Minor Radius	0.95	m
Toroidal Field	4.5	T
Plasma Current	2.7	MA
Duration	5-10	sec
Interval	10	min
Flux Swing	$\pm 13$	V-s
Net Heating Power	(NBI)	20 MW
	(LHRF)	7.5 MW
	(ICRF)	2.5 MW

**Table 2** Diagnostics and Monitors used in the initial experiments

- 1) 2 mm microwave interferometer (1 ch)
- 2) SX pulse height analyzer (PHA; 1 ch)
- 3) SX Surface Barrier Diode Array (4 ch)
- 4) Bolometer array (4 ch + 1 ch at divertor)
- 5) H $\alpha$  photo diode array (3 ch + 1 ch at divertor)
- 6) Visible color TV (radial view angle)
- 7) Electromagnetic sensors
- 8) Residual Gas Analyzer

Table 3 Preconditioning of vacuum vessel

- (1) Removal of dust in air by using a micron filter cleaner.
- (2) Spray of hot water by jet spray gun.
- (3) Spray of freon by jet spray gun.
- (4) Wiping of inner surfaces by special cloths wetted with acetone or freon
- (5) Bake out of vacuum vessel.
  - ① 1st('84/ 9/20~ 9/26 ) ~125 hours at 350 °C
  - ② 2nd('84/11/19~11/24 ) ~110 hours at 350 °C
  - ③ 3rd('85/ 2/13~ 2/24 ) ~260 hours at 250 °C

Table 4 Results of low current pulse discharge cleaning runs.

Item	Time (Hours)	Number of shots	Temperature of vacuum vessel
(1) 1st discharge cleaning ( '85/ 5 / 8 ~ 5/11 )	~30	~ 68,000	high temperature 150 ~200 °C
(2) 2nd discharge cleaning ( '85/ 5/13 ~ 5/17 )	~52	~106,000	room temperature 20 °C
(3) 3rd discharge cleaning ( '86/ 2/26 ~ 2/28 )	~23.5	~ 65,400	high temperature 150 ~200 °C



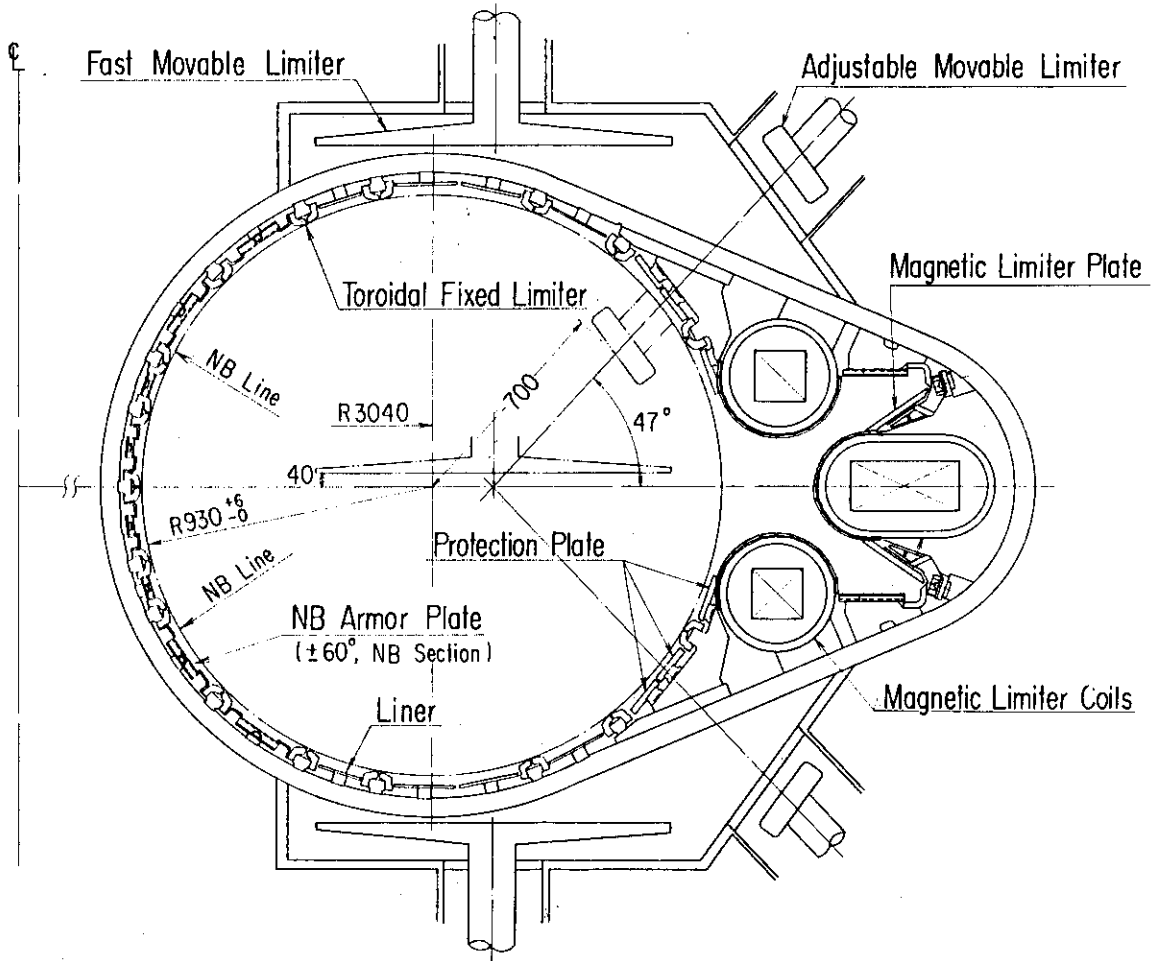


Fig. 1 Cross section of the JT-60 vacuum vessel<sup>9)</sup>.

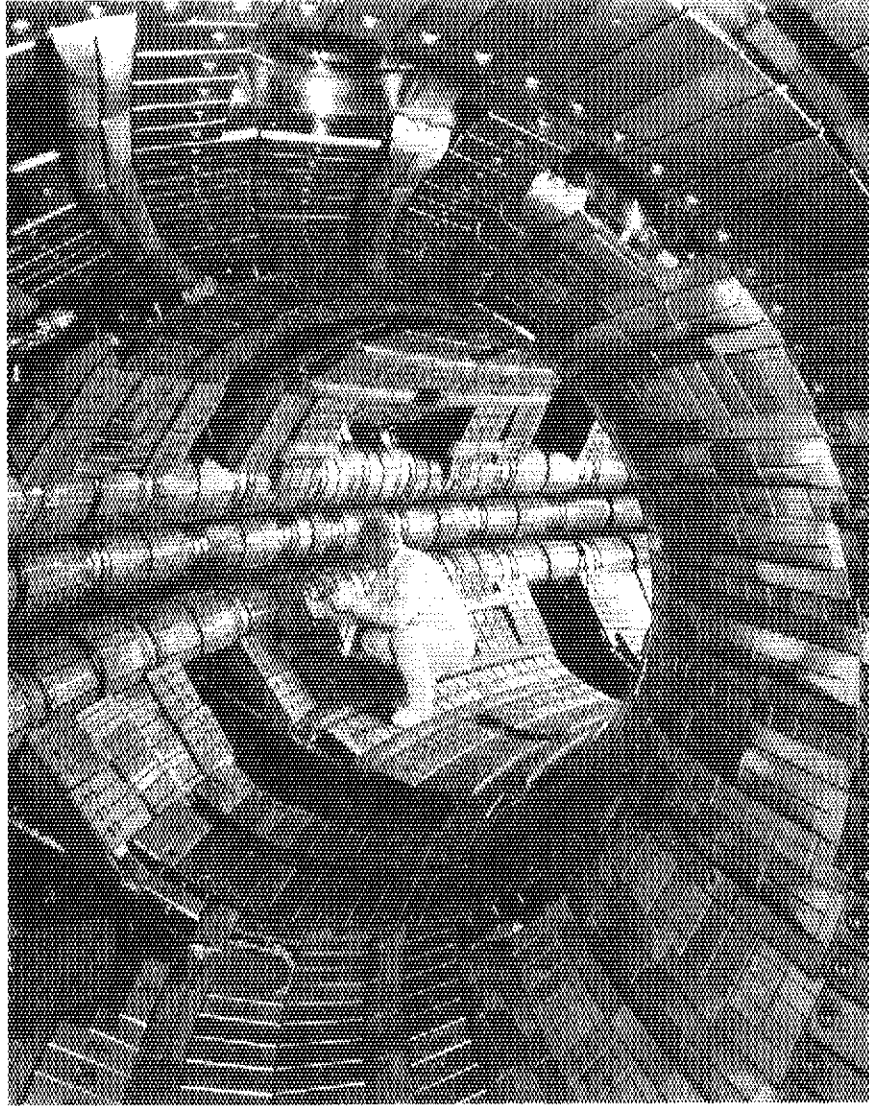


Fig. 2 Photograph of the inside of the JT-60 vacuum vessel prior to the first ohmic heating experiment.

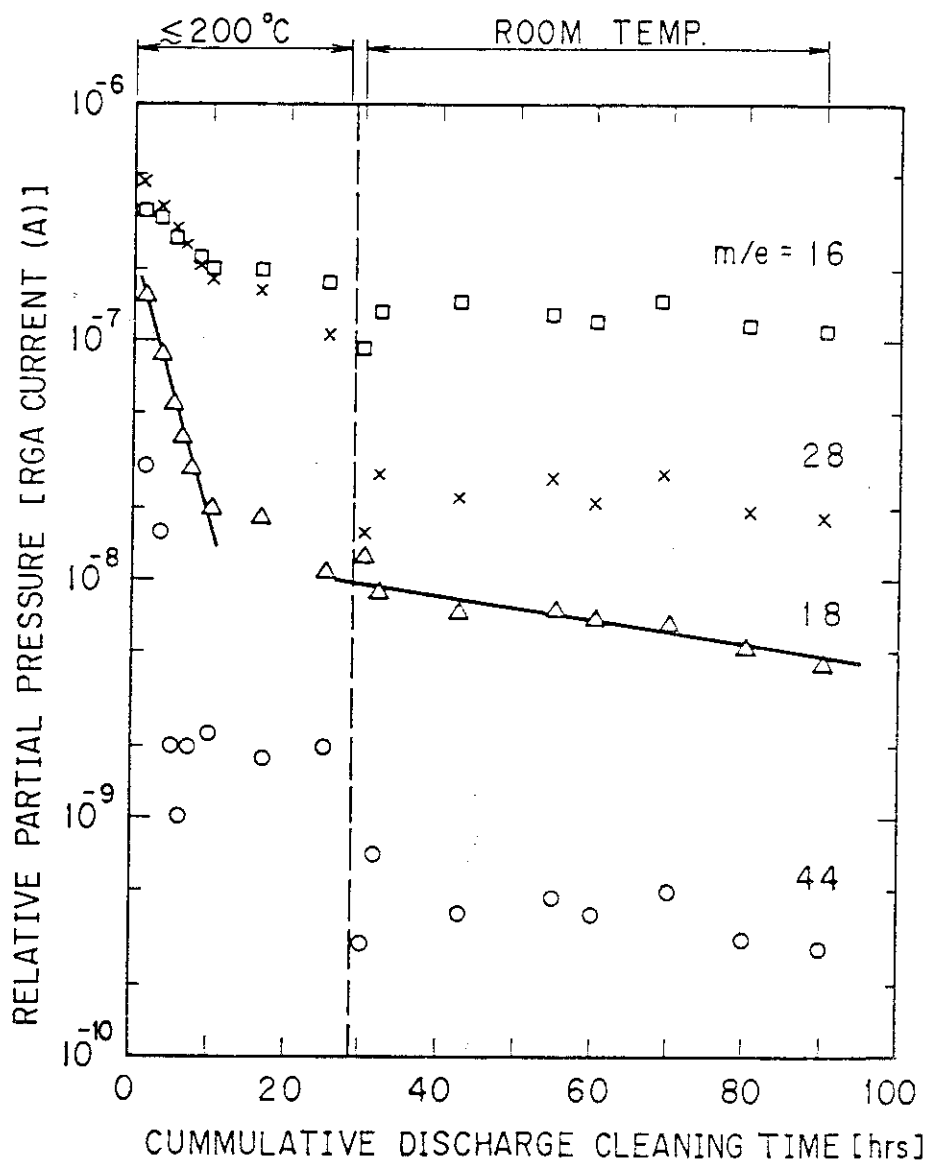


Fig. 3 Variation of residual gas analyzer signal during Taylor type discharge deaning<sup>24)</sup>.

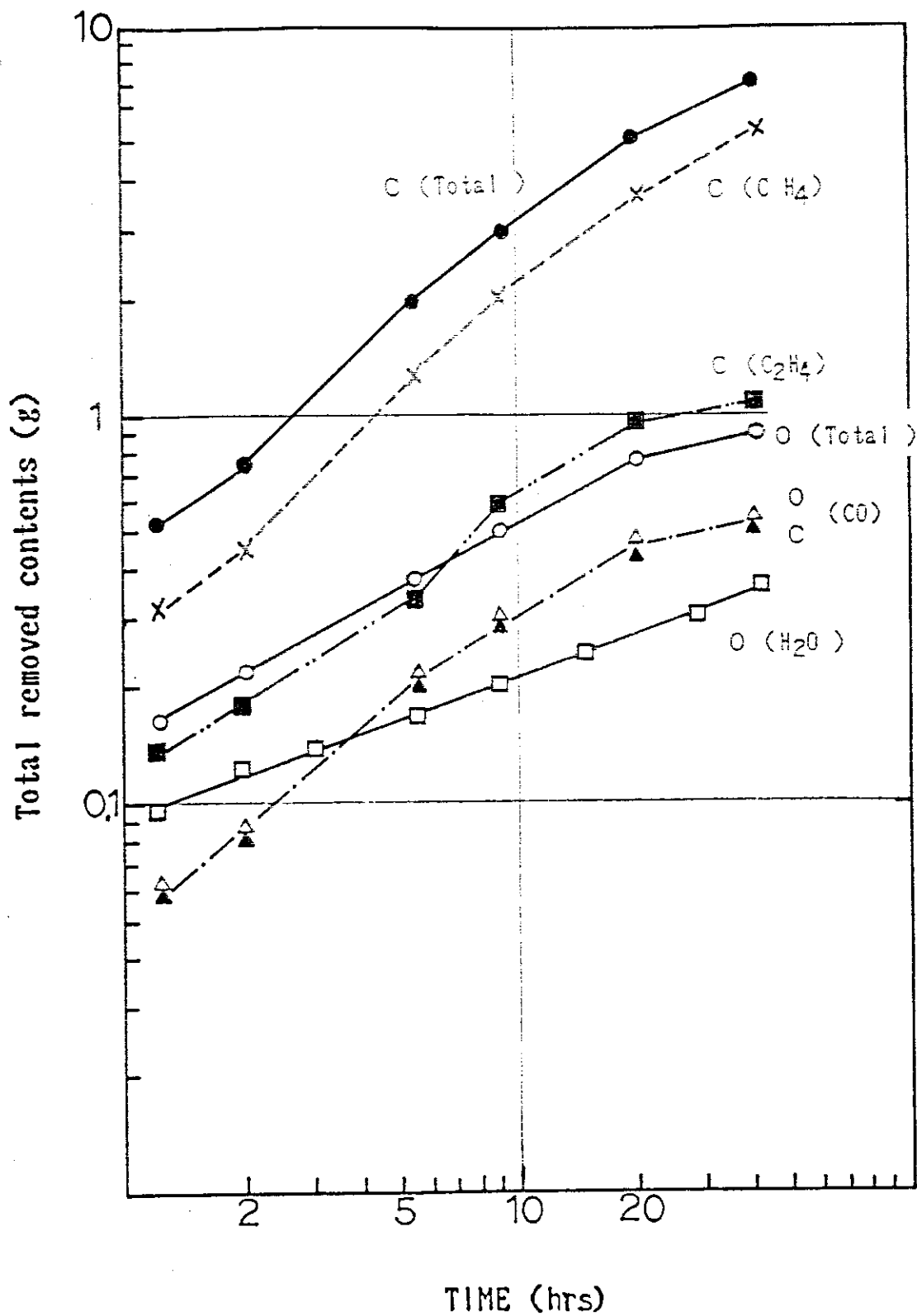


Fig. 4 Total removal contents during discharge cleaning<sup>24)</sup>.

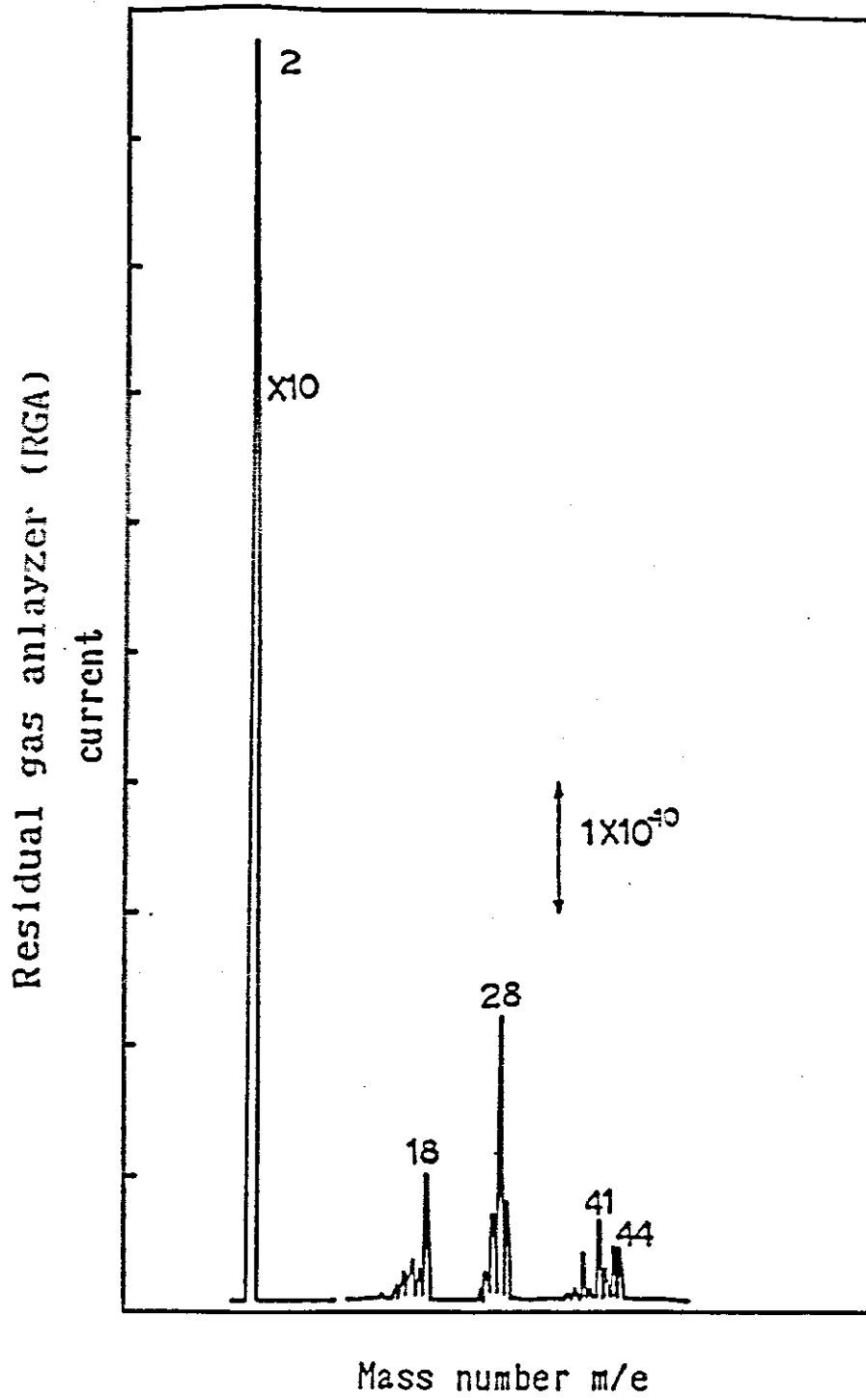


Fig. 5 Mass spectra of residual gas after 2nd discharge cleaning<sup>24)</sup>.

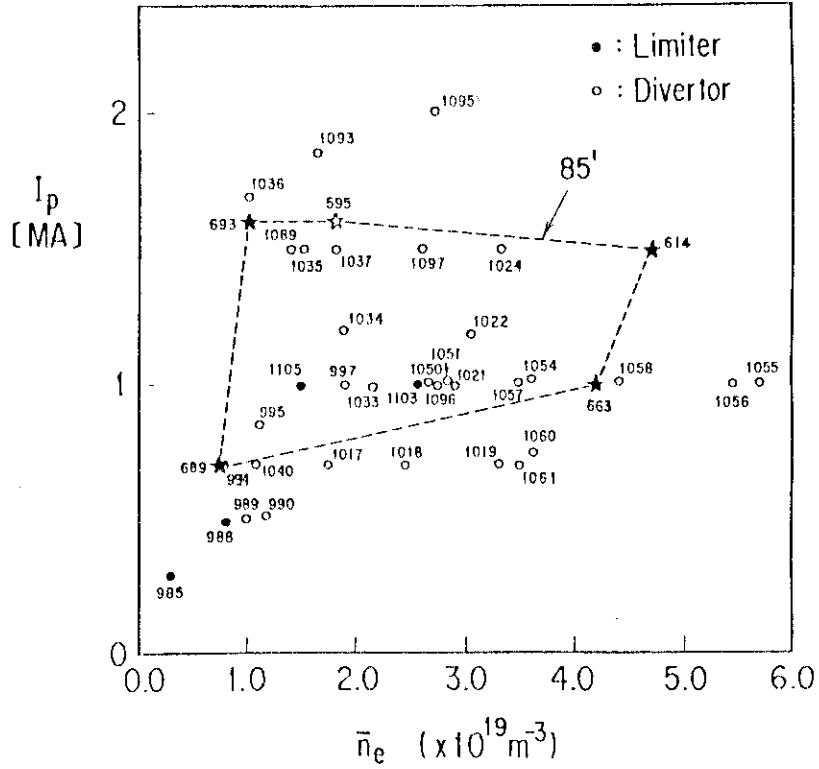


Fig. 6 Range of operating parameters for limiter and divertor discharges ( $I_p$  vs.  $\bar{n}_e$ ).

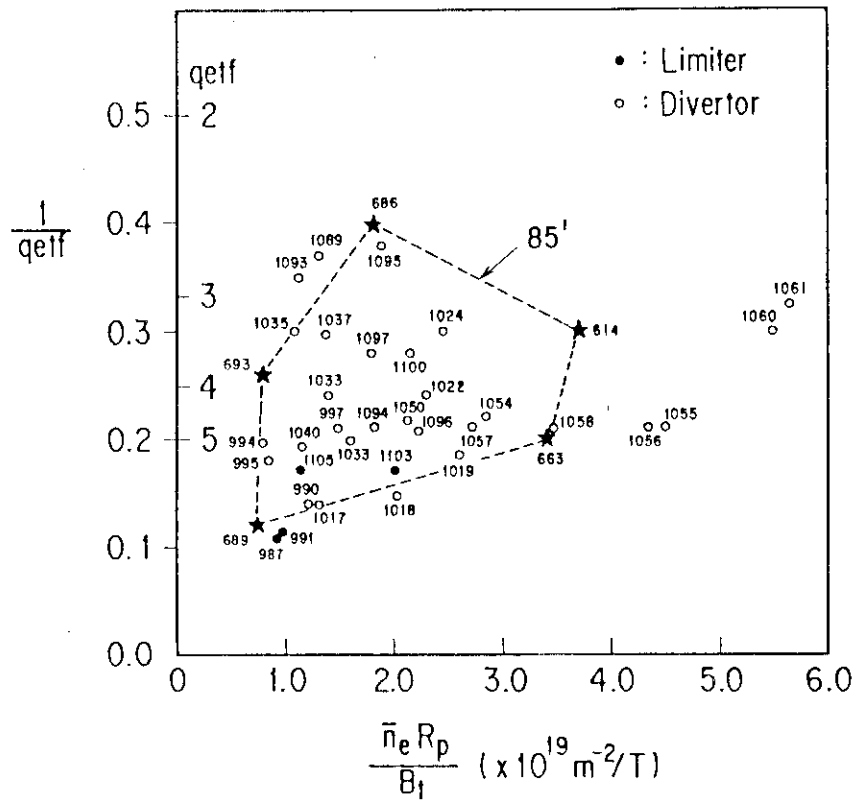


Fig. 7 Range of operating parameters for limiter and divertor discharges ( $1/q_{eff}$  vs. Murakami coefficient).

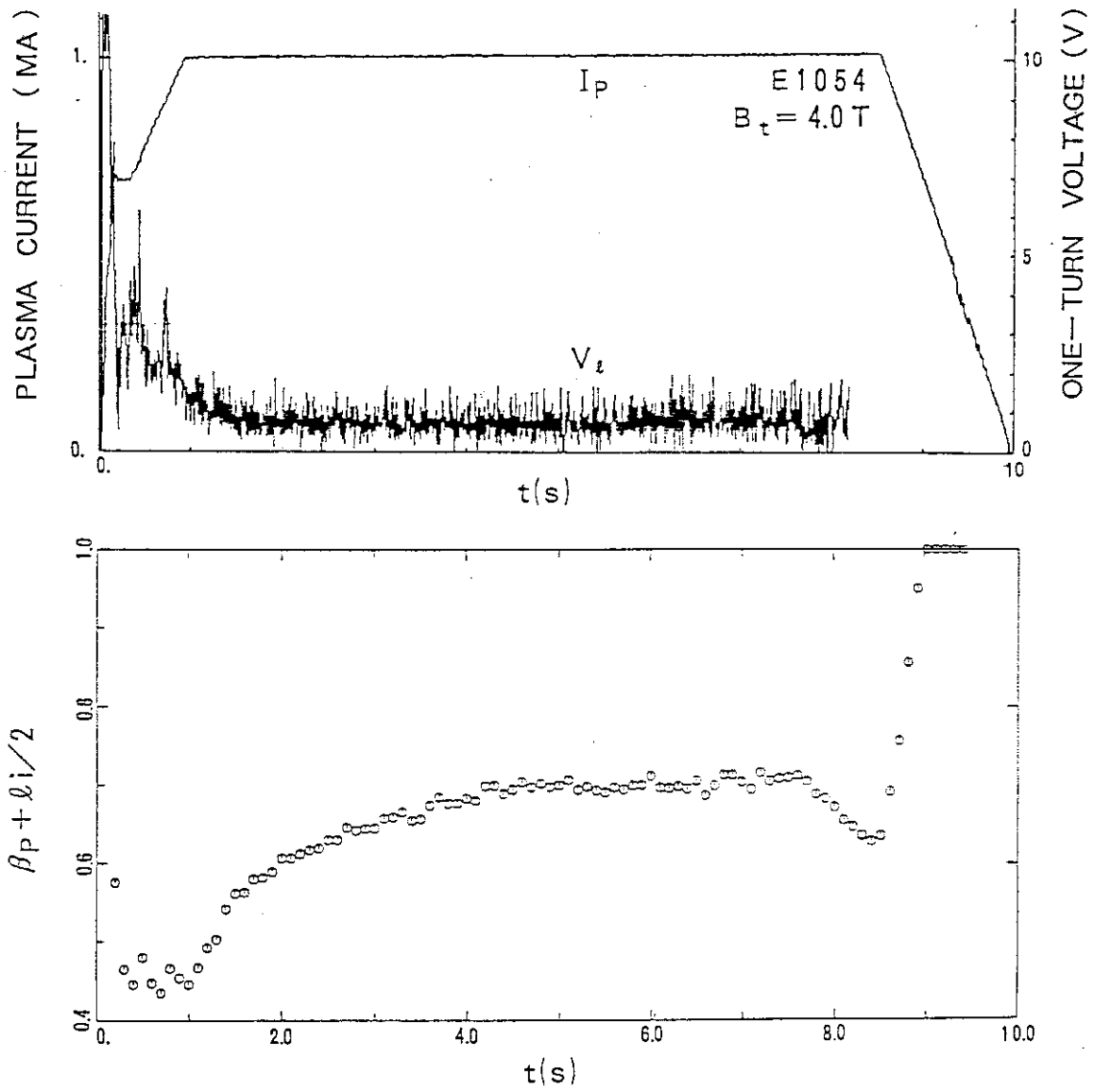


Fig. 8 Typical waveforms of 10 sec divertor discharge<sup>19)</sup>.

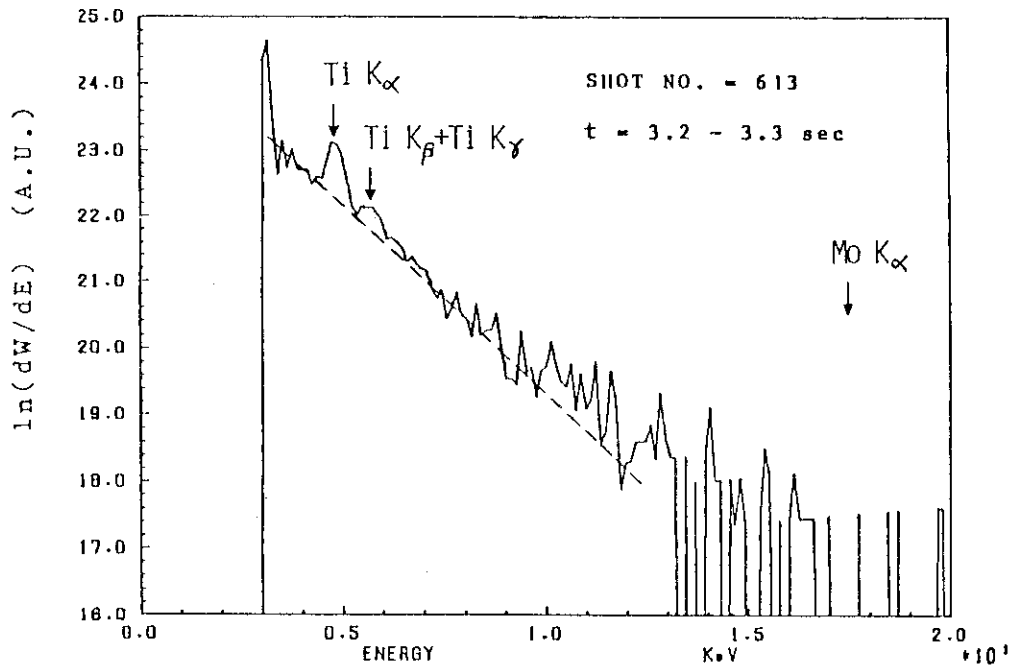


Fig. 9 Typical soft X-ray spectrum of a divertor discharge<sup>15)</sup>.

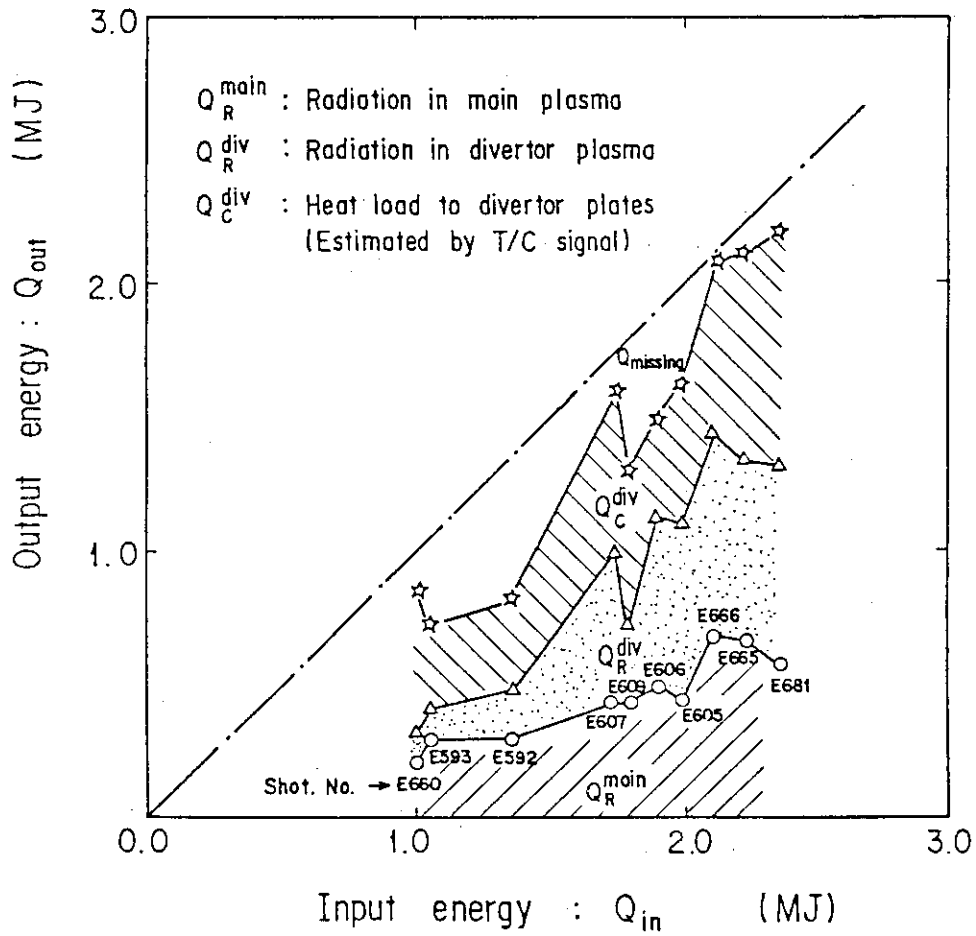


Fig. 10 Energy accounting of divertor discharges during the current flat top<sup>27)</sup>.



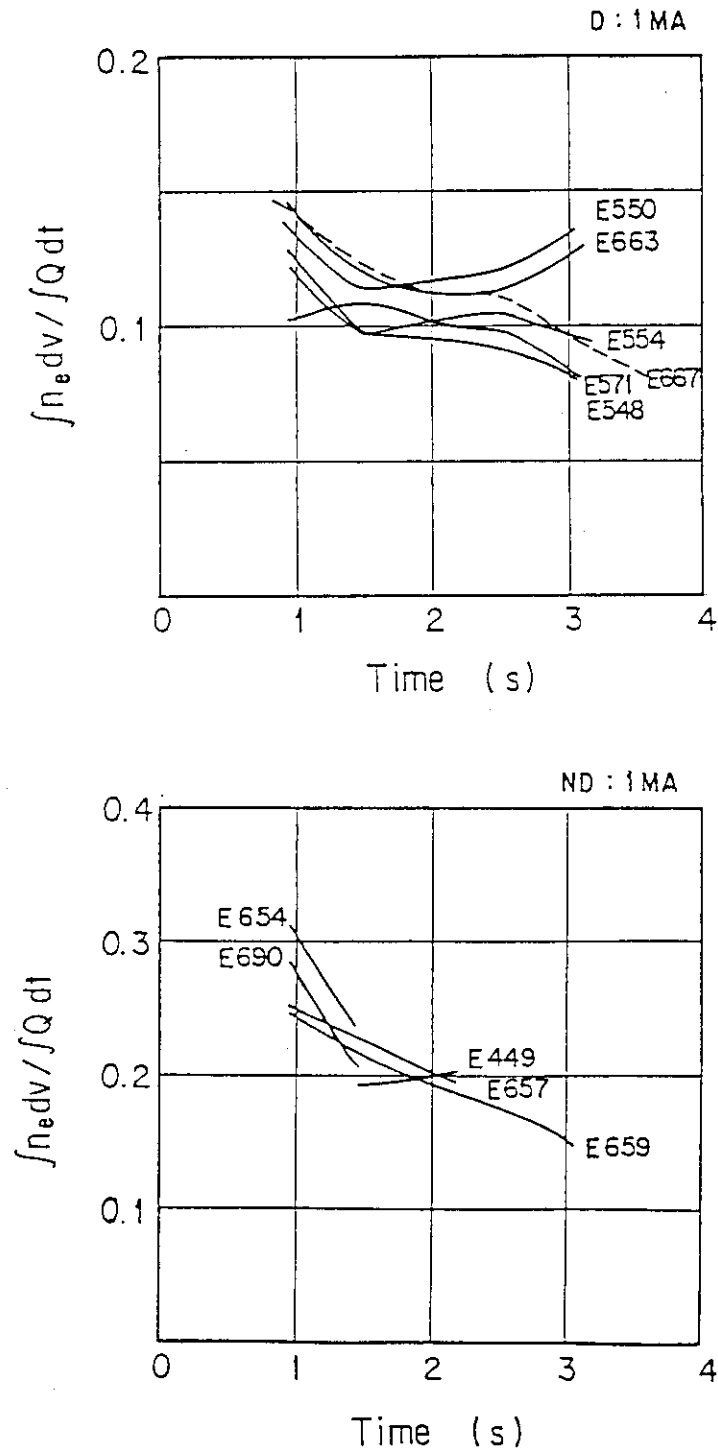


Fig. 11 Ratio of the total number of electrons in the plasma to that in the injected hydrogen gas<sup>15)</sup>.

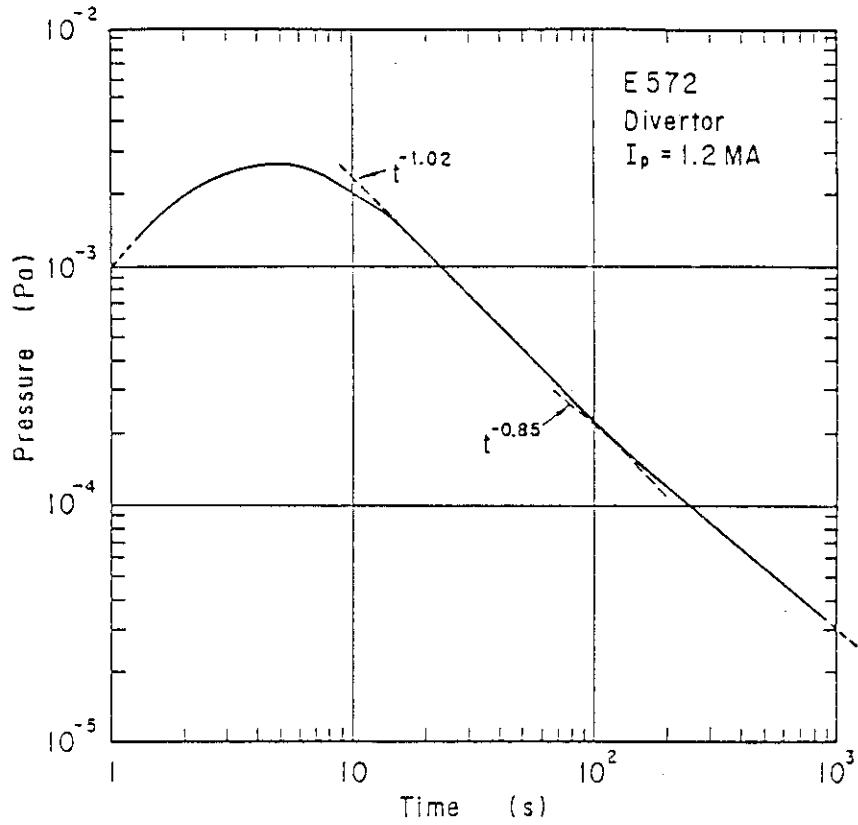


Fig. 12 Pressure change after a divertor discharge.

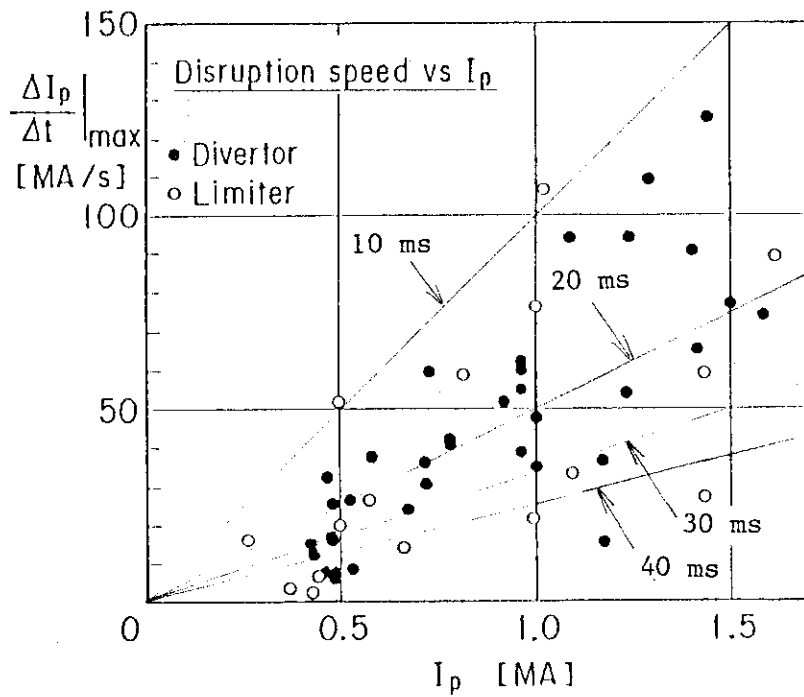


Fig. 13 Current decay rate of disruption.

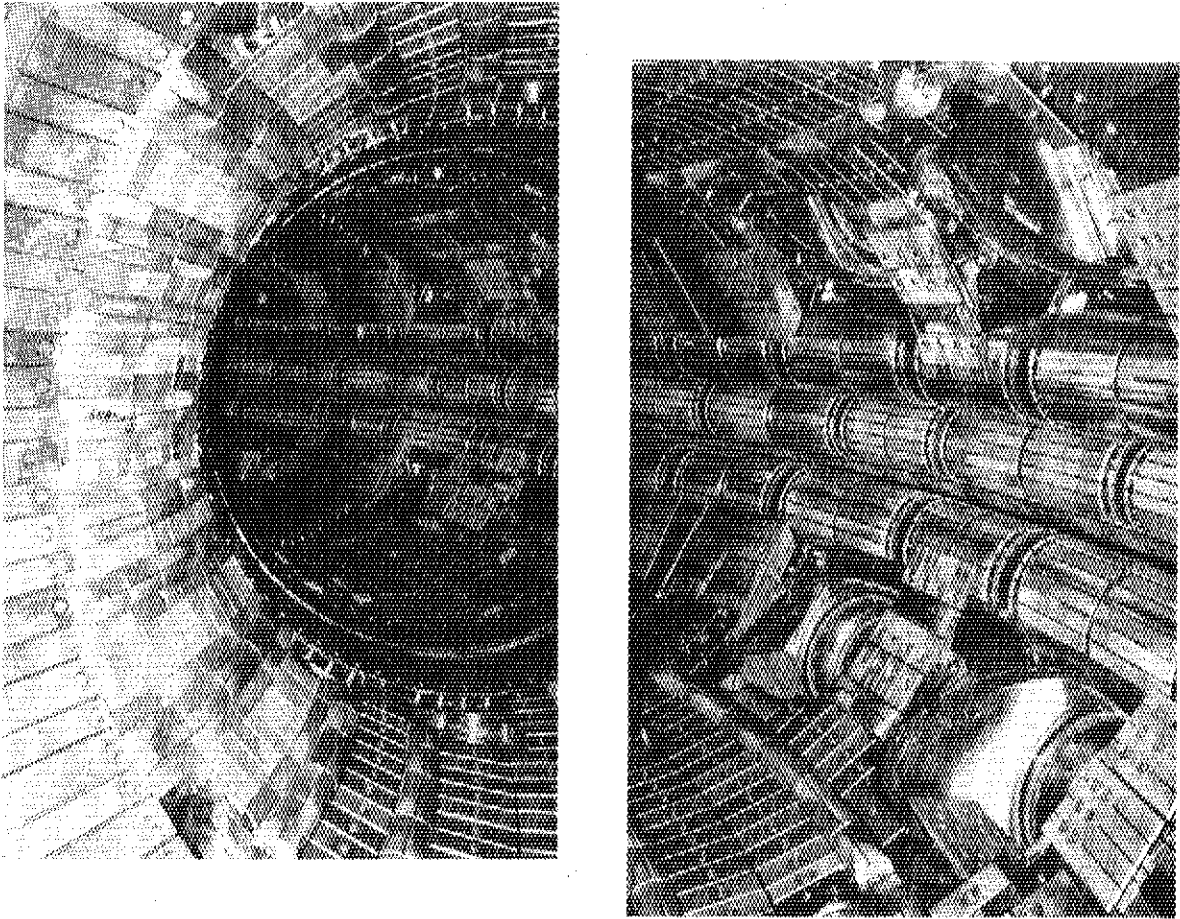


Fig. 14 Photograph of the inside of the JT-60 vacuum vessel after the first ohmic heating experiment during April-June 1985.

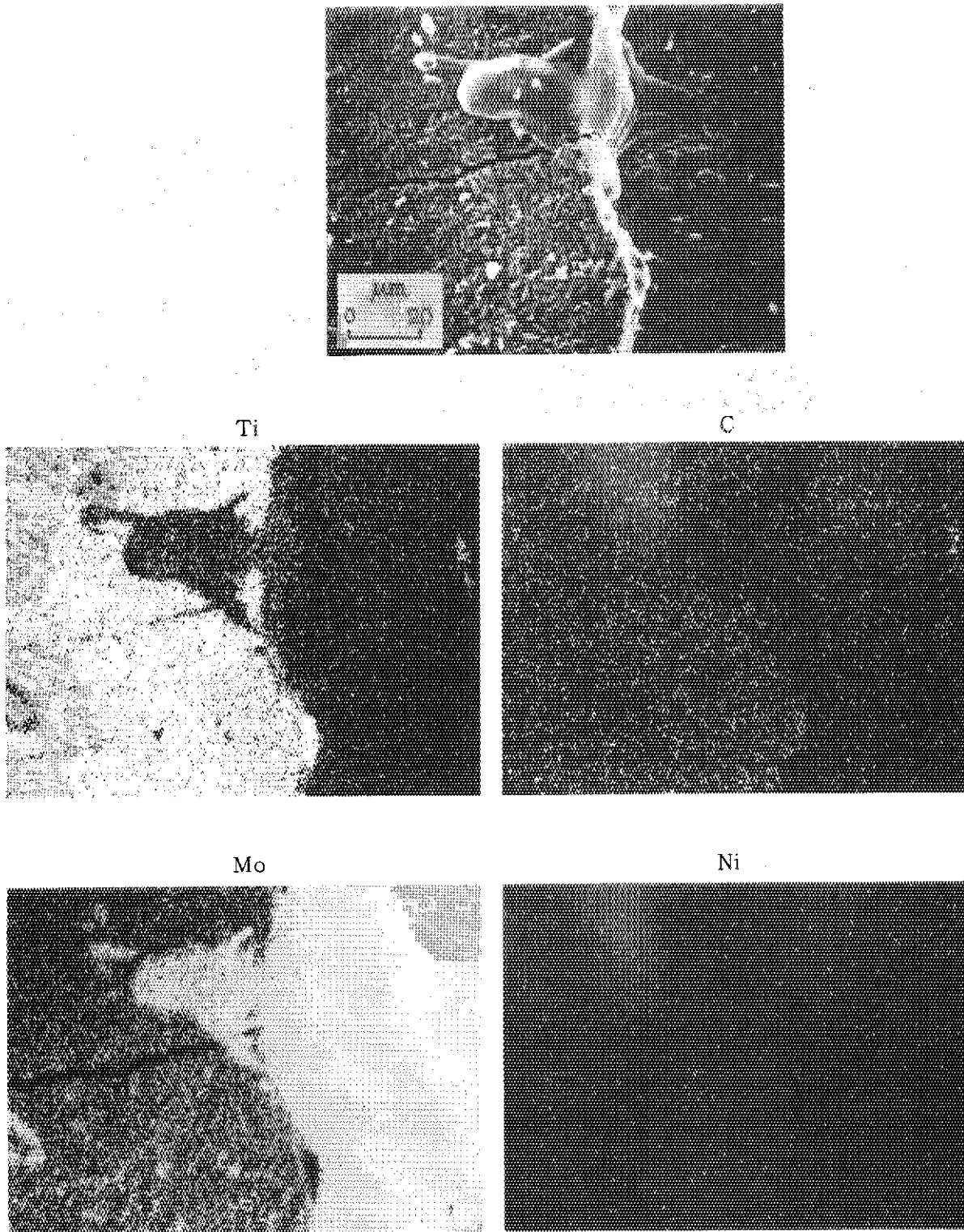


Fig. 15 SEM micrograph and EPMA X-ray image analysis of melted TiC coated Mo.

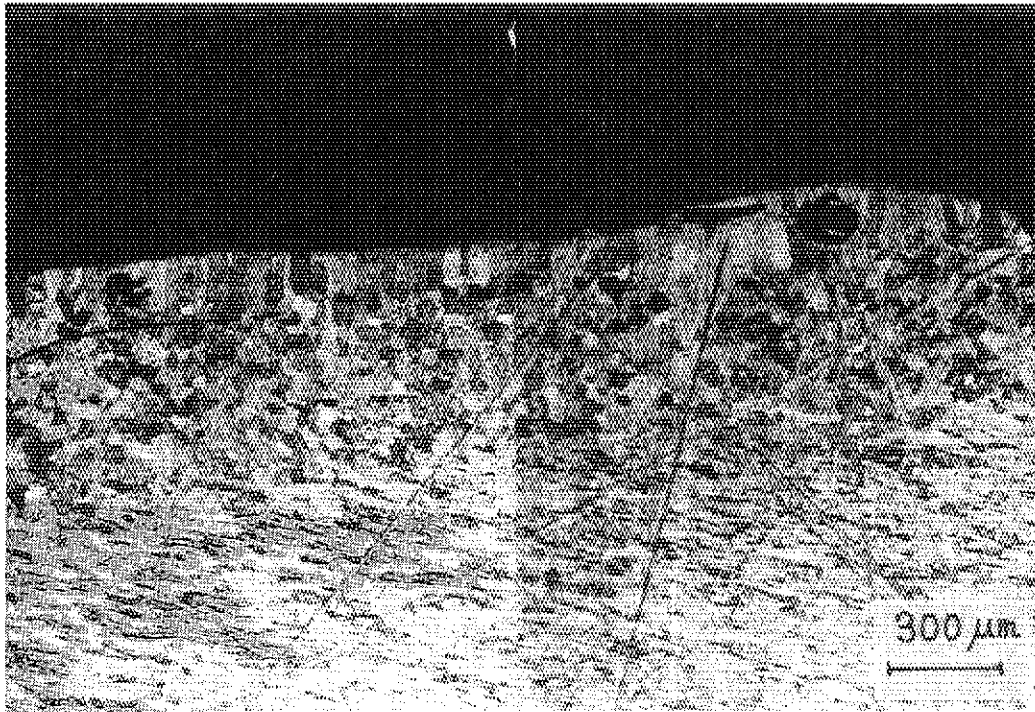


Fig. 16 Cross-section of melted zone in TiC coated Mo limiter.

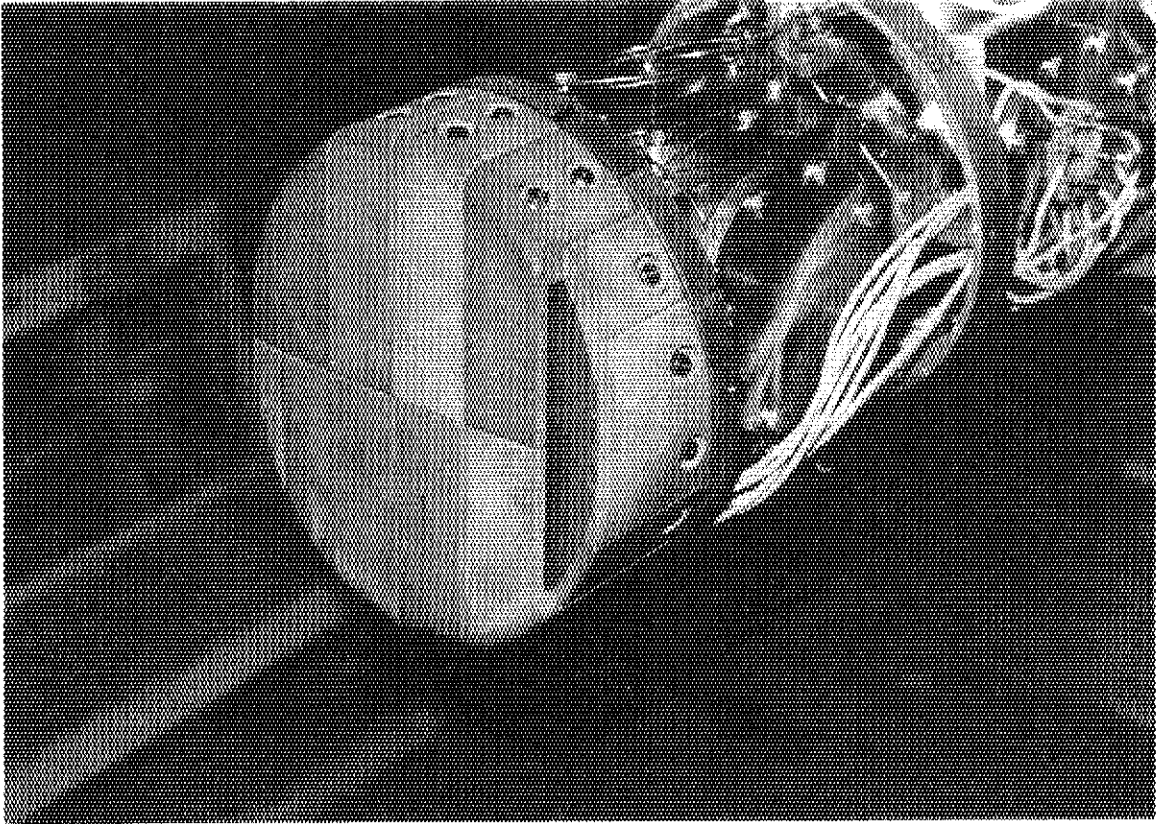


Fig. 17 Photograph of the module pump limiter head.

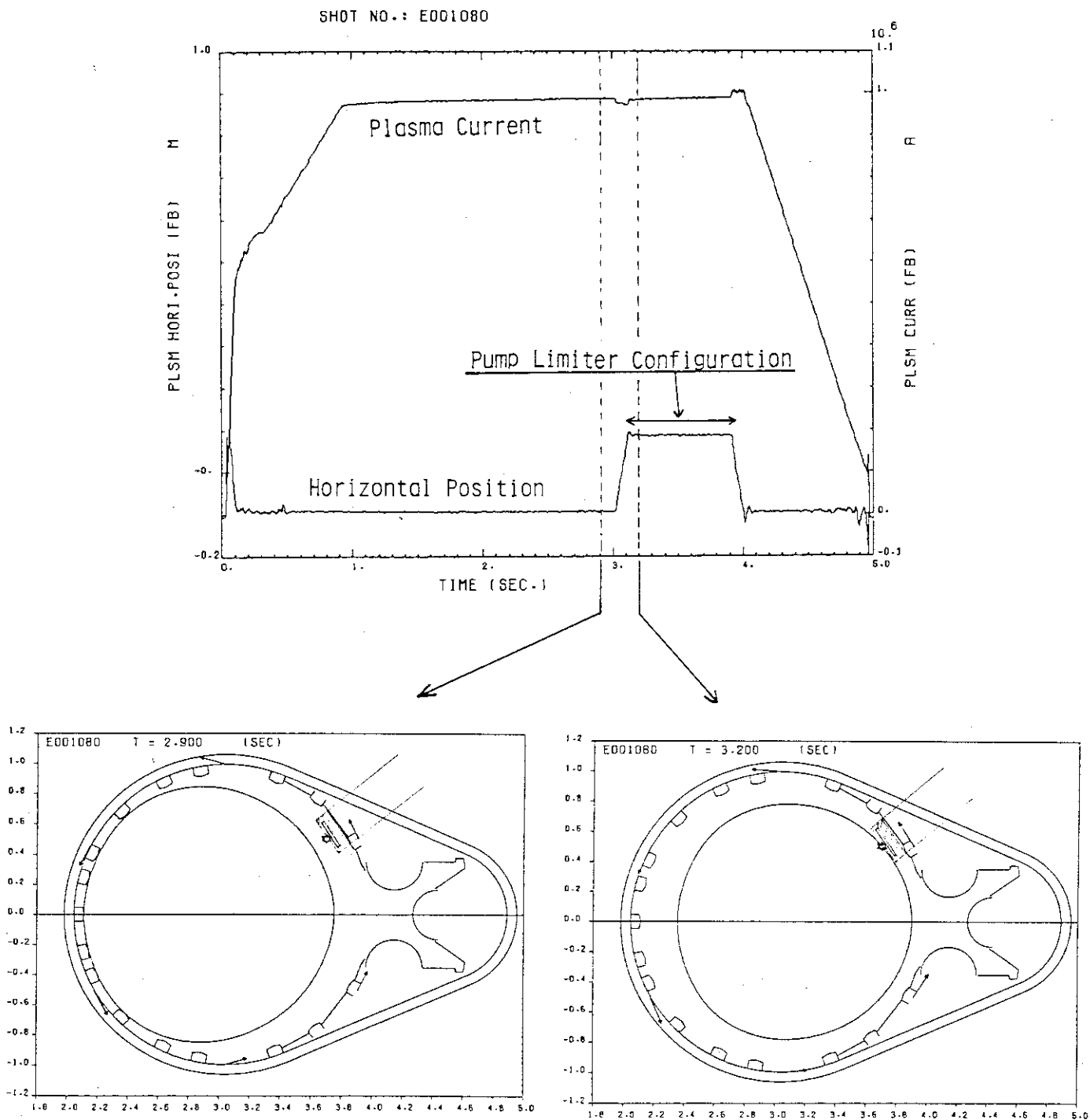


Fig. 18 Typical wave forms in the JT-60 pump limiter experiment.

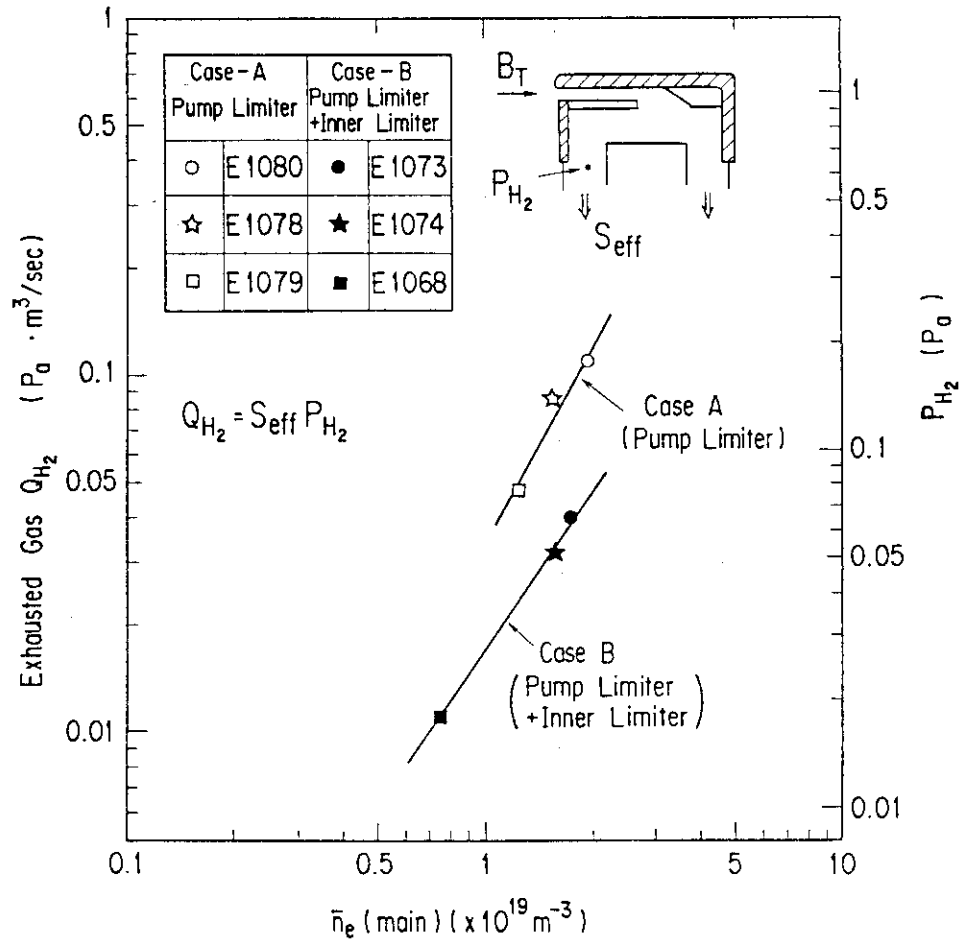


Fig. 19 Dependence of the limiter head pressure and gas exhaust rate in the pump limiter experiment.

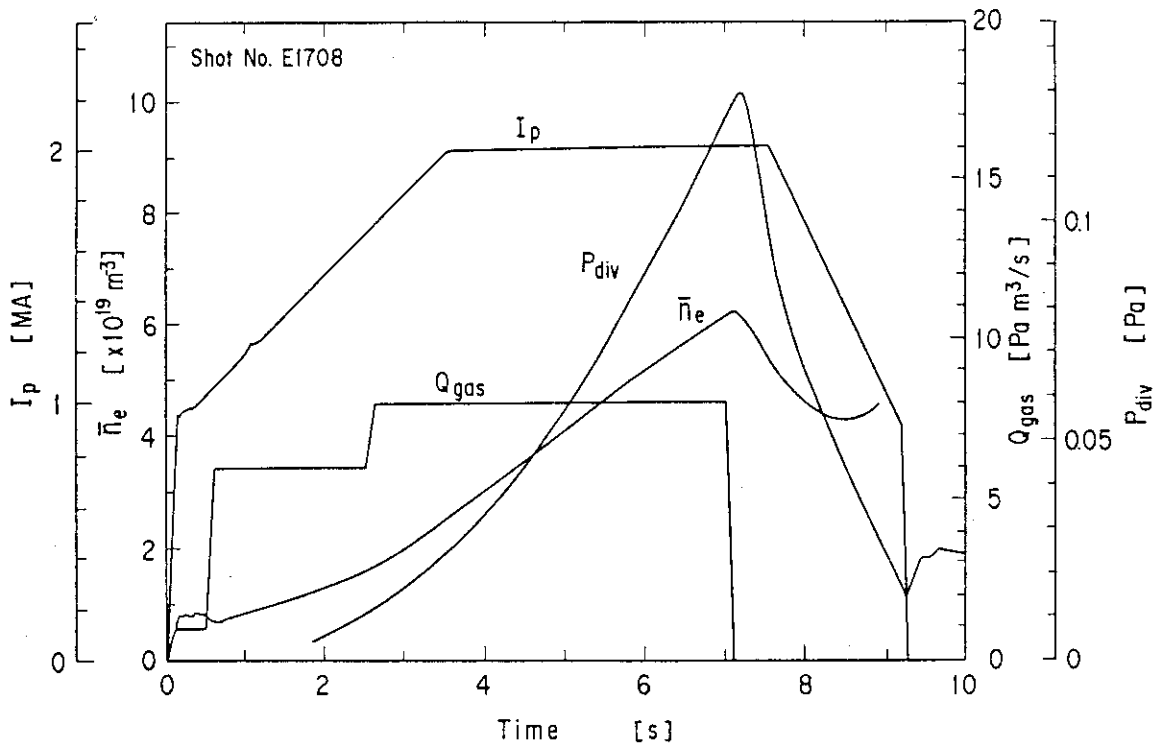


Fig. 20 Typical divertor discharge showing plasma current  $I_p$ , line averaged electron density  $\bar{n}_e$ , gas injection rate  $Q_{gas}$  and pressure in the divertor chamber  $P_{div}$ .<sup>23)</sup>



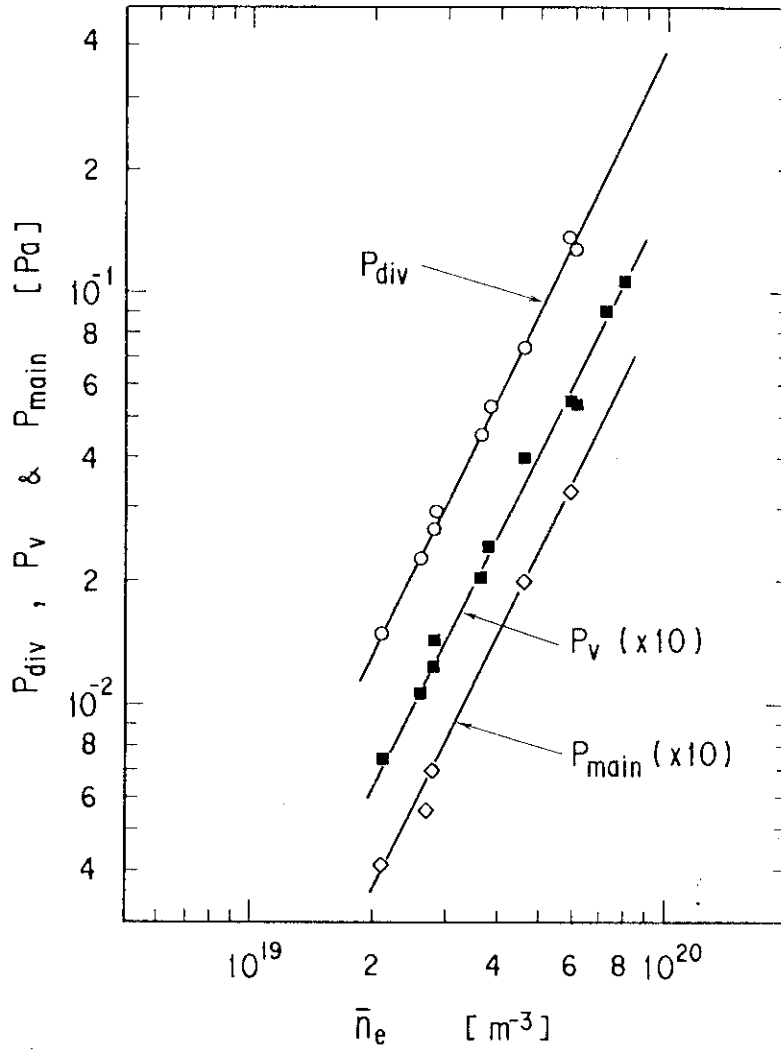


Fig. 21 Pressures in the divertor chamber  $P_{\text{div}}$ ,  
in the main chamber.<sup>23)</sup>

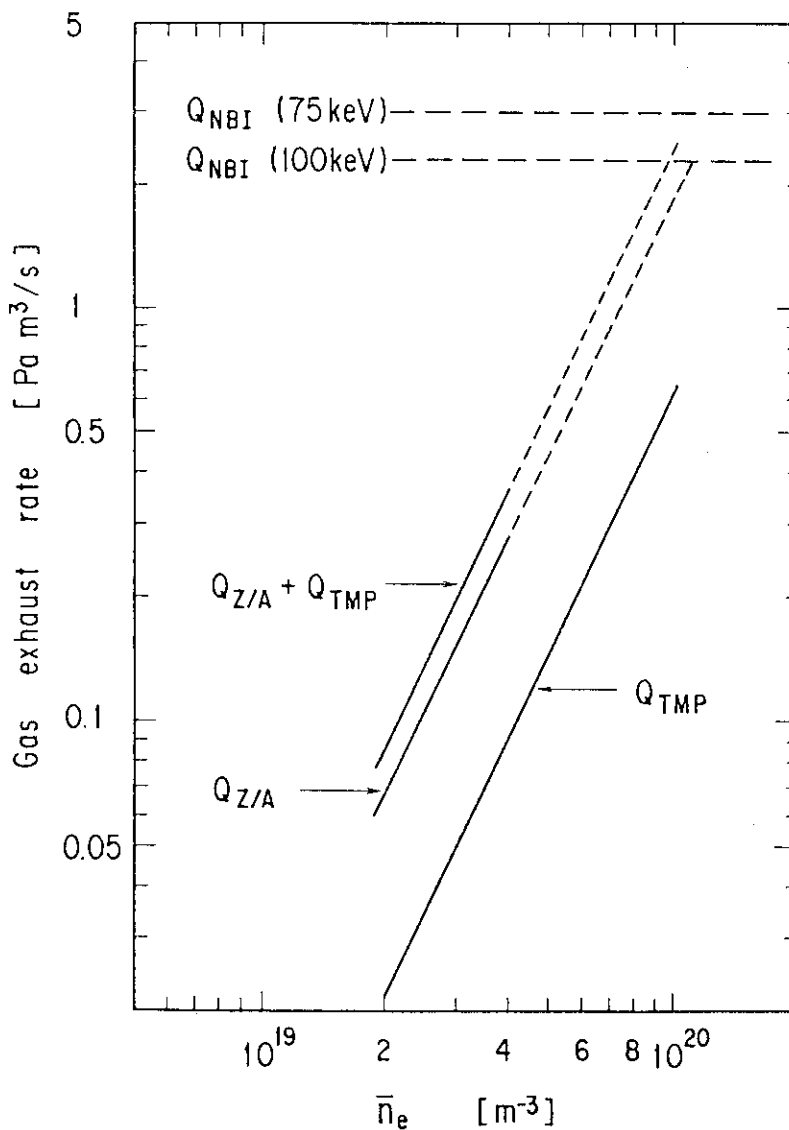


Fig. 22 Gas exhaust rates of the getter pumps  $Q_{Z/A}$  and the torus main pumps  $Q_{TMP}$  vs.  $\bar{n}_e$ . Fueling rates by the neutral beam injection are also shown.<sup>23)</sup>